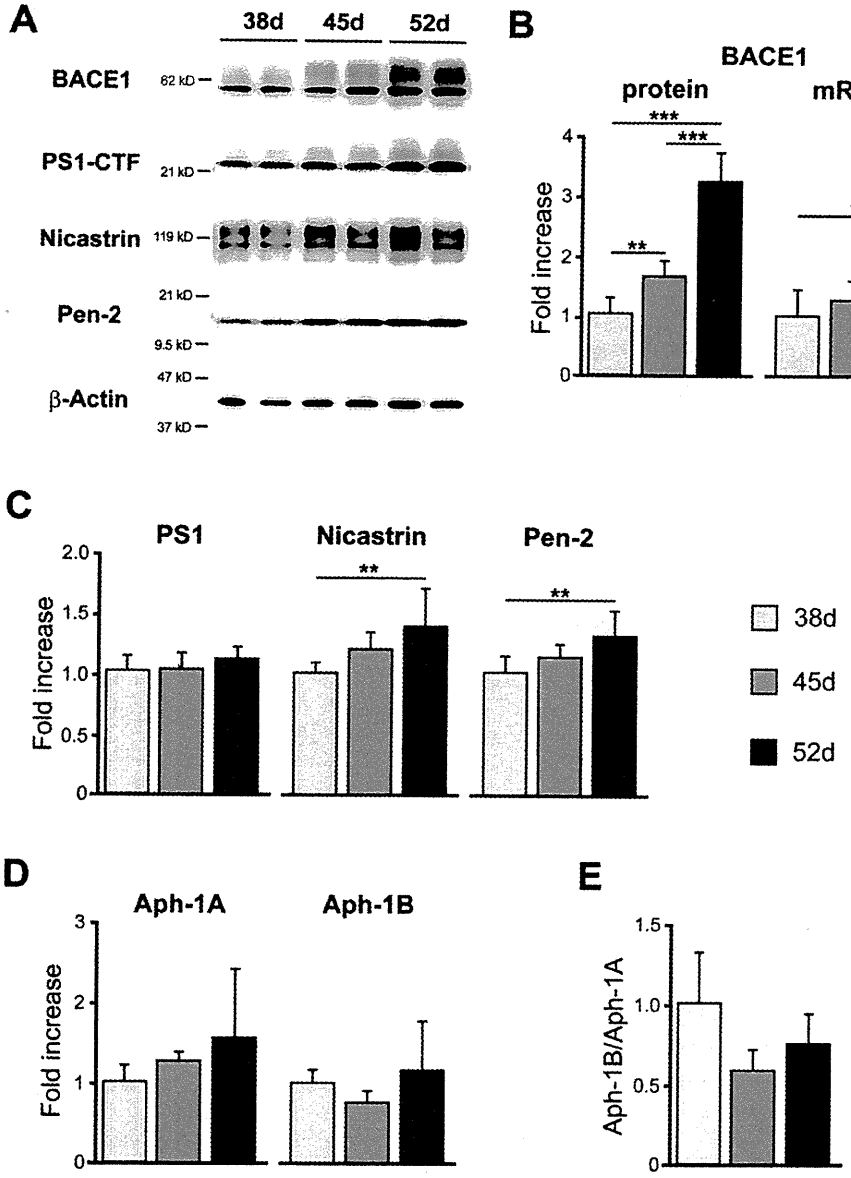

Figure 4. β-Secretase and γ-secretase components were expressed in hiPS cell-derived neuronal cells. The hiPS cell-derived neuronal cells express BACE1 protein and mRNA (B), γ-secretase components; presenilin 1(PS1), nicastrin, Pen-2 (C), and Aph-1A, and Aph-1B (D) at days 38, 45, and 52. Expression levels were quantified by western blot analysis (n = 8) (B, C) or qPCR (n = 3) (D) and normalized by that of β-actin. "Fold expression" represents the ratio of expression on the given day compared to day 38. (E) The ratio Aph-1B/Aph-1A. Data represent mean ± SD. (A) Representative western blots of BACE1 and γ-secretase components at 38, 45, and 52 days. $^{*}p<0.05$, $^{**}p<0.01$, $^{***}p<0.001$, Tukey's test.
doi:10.1371/journal.pone.0025788.g004

cells. APP, sAPPβ, APP-CTFβ and BACE1 protein levels were increased (Figures 3 and 4), but protein levels of γ-secretase components were not significantly different during the period from day 38 to 52 (Figure 4C, D). Aβ production in hiPS cell 253G4-derived neuronal cells increased with differentiation course (Figure 5A), however that in another hiPS cell 201B7 [5]- and in hES H9-derived neuronal cells did not increase (Figures S5 and S7) although all cell lines showed development of synapse (Figure S4A) as Aβ releasing site [41], indicating that besides synaptogenesis, subtle changes in localization and assembly of APP [42], BACE1, γ-secretase components would be critical for Aβ production.

The Aβ42/Aβ40 ratio unexpectedly showed a significant decrease from day 38 to 45 (Figure 5B). Serneels *et al.* reported that the γ-secretase complex containing Aph-1B was active and involved in the generation of amyloidogenic Aβ42 [24]. Our data showed that the Aph-1B/Aph-1A ratio did not change significantly with cell differentiation (Figure 4E); therefore, the Aβ42/Aβ40 ratio may be influenced by other unknown factors interacting directly or indirectly with γ-secretase.

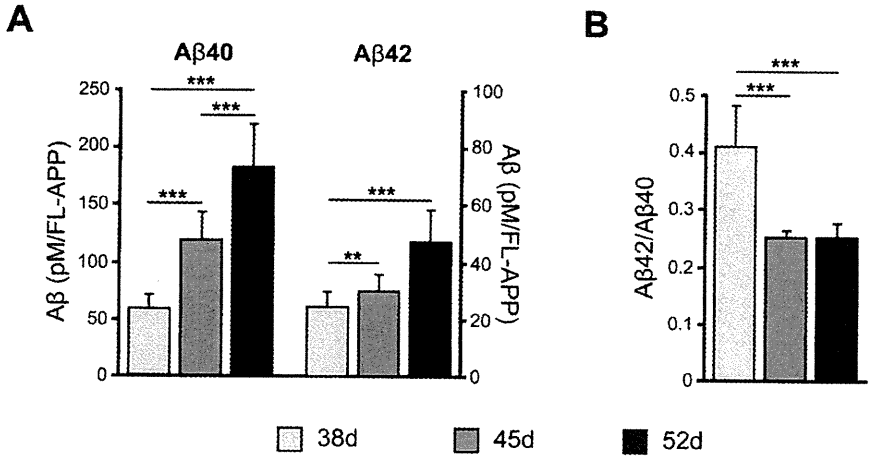

Figure 5. Aβ was produced in hiPS cell-derived neuronal cells. (A) Aβ40 or Aβ42 secreted into the conditioned media and FL-APP were measured by sandwich ELISA and western blot analysis, respectively. Expression level of Aβ was normalized by that of FL-APP. (B) Aβ42/Aβ40 ratios. Data represent the mean ± SD of 8 assays. *, #$p<0.05$, **, ##$p<0.01$, ***, ###$p<0.001$, Tukey's test.
doi:10.1371/journal.pone.0025788.g005

BSI, GSI, and the NSAID sulindac sulfide inhibited Aβ production in this human neuronal cell system (Figure 6). The inhibitory effect on Aβ production by GSI showed a characteristic difference between days 38 (Aβ surge) and 52 (gradual Aβ rise) (Figure 6C, D). Aβ surge at day 38 was also observed in another hiPS cell (201B7)-derived neuronal cells (Figure S7) as well as in hES cell line, H9-derived ones (Figure S5). At day 38, GSI might promote neuronal differentiation with synaptogenesis via blocking Notch signaling [43] rather than inhibition of Aβ production, leading to Aβ surge. Another possible explanation for Aβ surge is that change in conformation or components of the γ-secretase affects the sensitivity of γ-secretase to GSI (total Aβ, Aβ40, Aβ42, and Aβ42/Aβ40), although levels of mRNA and the ration for Aph-1A and Aph-1B do not change between days 38 and 52 (Figure 4D, E) Thus, for precise Aβ monitoring in human stem cell-derived neuronal cells, it is necessary to use neuronal cells with a sufficient substrate level and synaptogenesis, because Aβ is released presynaptically, as mentioned above.

Some NSAIDs are known to preferentially lower Aβ42 [33,34]. Our data showed that sulindac sulfide was capable of inhibiting Aβ42 secretion at high concentrations ($\geq 10^{-5}$ M) (Figure 6F), although a few NSAIDs do not show therapeutic effects for AD. Negative results might be due to low γ-secretase modulator potency [44]. To discover novel effective drugs for modulating β- or γ-secretase activity, the *in vitro* hiPS cell-derived neuronal cell assay system might be expected to yield such drugs.

Familial AD patient specific neuronal cells generated by direct conversion (induced neuron, iN) show higher Aβ42/Aβ40 ratio than those of unaffected individuals [45]. Based on this report, hiPS/hES cell-derived neurons expressing mutant PS1, PS2, or APP may show higher Aβ42/Aβ40 ratio. Comparing to our results, the levels of Aβs in this assay (Aβ40; ~1.7 ng/ml at day 52) is higher than that using iN cells (Aβ40; ~0.1 ng/ml), although iN cells become functional neurons more quickly. The optimization of neuronal cell condition for comparison of the Aβ42/Aβ40 ratio between multiple iPS cell-derived neuronal cells may be required.

In conclusion, our findings indicate that hiPS cell-derived neuronal cells express functional β- and γ-secretases related to the production of Aβ in the present experimental conditions. In addition, our data provide the proof in principle that hiPS cell-derived neuronal cells can be applied to drug screening and AD patient-specific iPS cell research.

Materials and Methods

Antibodies and reagents

Primary antibodies used were as follows: mouse anti-Nestin (1:200, Millipore, Temecula, CA), mouse anti-Tuj1 (1:2000, Covance, Princeton, NJ), rabbit anti-GFAP (1:500, DAKO, Carpinteria, CA), rabbit anti-Synapsin I (1:500, Millipore), mouse anti-Cux1 (1:100, Abnova, Taipei, Taiwan), rabbit anti-Satb2 (1:1000, Abcam, Cambridge, UK), rat anti-Ctip2 (1:500, Abcam), rabbit anti-Tbr1 (1:500, Abcam), rabbit anti-vGlut1 (1:1000, Synaptic Systems, Göttingen, Germany), rabbit anti-Foxg1 (1:100, Abcam), rabbit anti-GABA (1:1000, Sigma-Aldrich, St. Louis, MO), rabbit anti-GAD65/67 (1:200, Millipore), mouse anti-PAG [46] (1:500), rabbit anti-APP (1:15000, Sigma-Aldrich), mouse anti-APP (1 μg/ml, Millipore), rabbit-anti BACE (1:2000, Merck, Darmstadt, Germany) mouse anti-PS1 loop C-terminus (1:1000, Millipore), rabbit anti-nicastrin (1 μg/ml, Thermo Scientific, Rockford, IL), rabbit anti-Pen-2 (1:1000, Invitrogen, San Diego, CA), mouse anti-MAP2 (1:200, Millipore), goat anti-ChAT (1:100, Millipore), guinea pig anti-VAChT (1:500, Millipore), and mouse anti-β-actin (1:15000, Sigma-Aldrich). We raised rabbit polyclonal antibodies against the carboxyl terminals of human sAPPα (hsAPPα) and sAPPβ using the KLH-conjugated synthetic peptides CRHDSGYEVHHQK and CKTEEISEVKM, respectively (Figure S3). All animal experiments were performed in compliance with the institutional guidelines at RIKEN Brain Science Institute, and were approved by the Animal Care and Use Committee (Permit number: H17-2B031). Each antibody was purified with a peptide-conjugated column [47]. Alexa Fluor 488 and Alexa Fluor 594-conjugated secondary antibodies (Invitrogen) were used for immunofluorescence.

The β-secretase inhibitor IV [31] and γ-secretase inhibitor XXI/Compound E [32] were purchased from Merck. Sulindac sulfide (NSAID) was purchased from Sigma-Aldrich.

Immunocytochemistry

Cells were fixed with 4% paraformaldehyde in phosphate buffered saline (PBS) for 30 min, and incubated in PBS

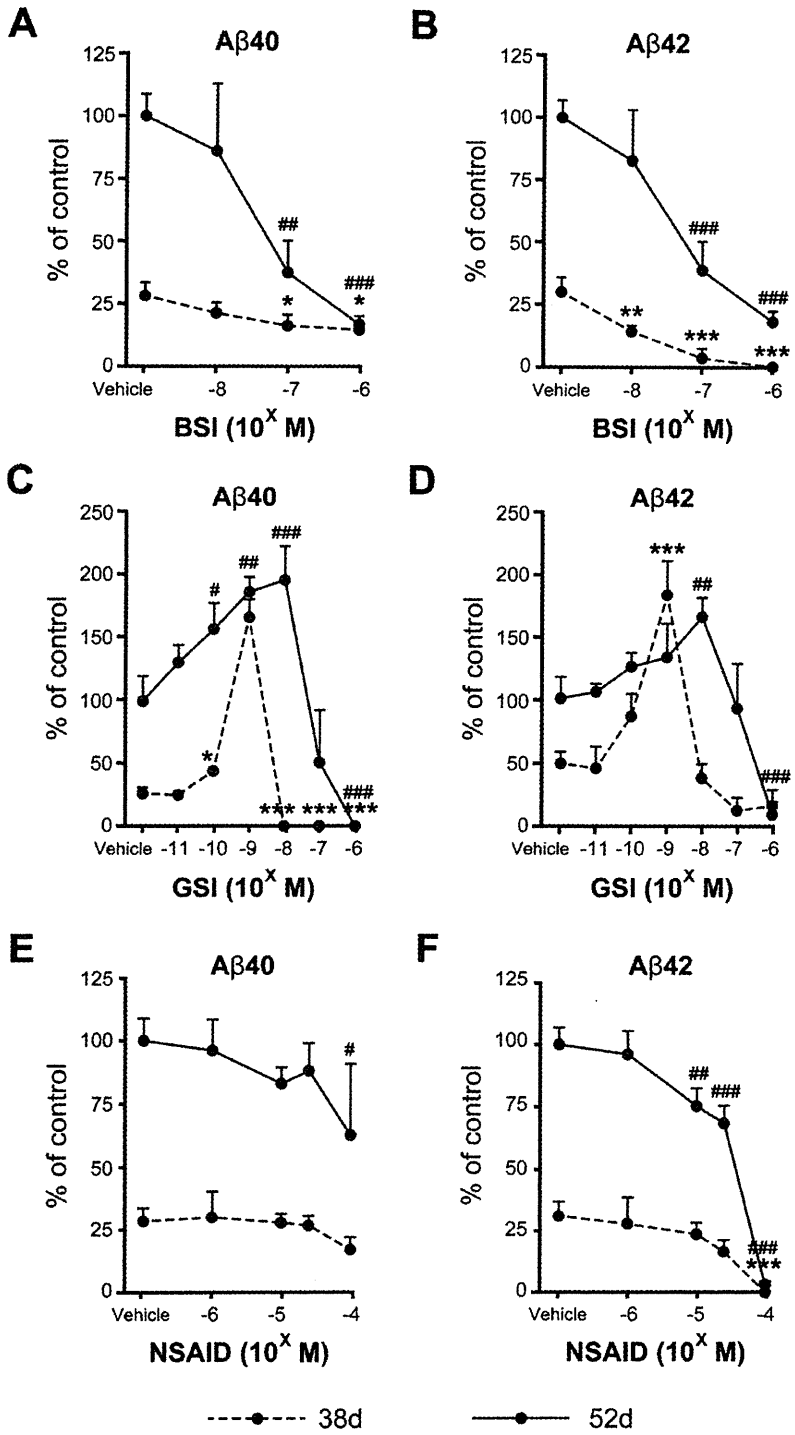

Figure 6. Aβ production was modulated by β- and γ-secretase inhibitors and an NSAID. β-Secretase inhibitor (BSI) (A, B), γ-secretase inhibitor (GSI) (C, D), and NSAID (E, F) were added into hiPS cell-derived neuronal cell cultures at day 36 (dotted line) and 50 (bold line), and two days later amounts of Aβ40 and Aβ42 secreted into the conditioned media were measured. The ratios Aβ40/FL-APP and Aβ42/FL-APP are expressed as percentages of the vehicle-treated group at day 52 and represent mean ± SD of 3 assays. A, B: There were significant main effects of day ($F(1, 16) = 72.5$ and 162.4, $p<0.001$ in Aβ40 and Aβ42, respectively) and dose ($F(3, 16) = 23.1$ and 45.7, $p<0.001$ in Aβ40 and Aβ42, respectively), and significant interaction between day and dose ($F(3, 16) = 13.0$ and 11.7, $p<0.001$ in Aβ40 and Aβ42, respectively) by 2-way ANOVA. C, D: There were significant main effects of day ($F(1, 28) = 240.5$ and 59.1, $p<0.001$ in Aβ40 and Aβ42, respectively) and dose ($F(6, 28) = 70.8$ and 37.8, $p<0.001$ in Aβ40 and Aβ42, respectively), and significant interaction between day and dose ($F(6, 28) = 23.5$ and 15.1, $p<0.001$ in Aβ40 and Aβ42, respectively) by

2-way ANOVA. E, F: There were significant main effects of day ($F(1, 20) = 196.9$ and 418.0, $p<0.001$ in Aβ40 and Aβ42, respectively) and dose ($F(4, 20) = 4.16$, $p=0.013$ and $F(4, 20)=91.9$, $p<0.001$ in Aβ40 and Aβ42, respectively), and significant interaction between day and dose ($F(4, 20)=25.4$, $p<0.001$ in Aβ42) by 2-way ANOVA. *, $^{\#}p<0.05$, **, $^{\#\#}p<0.01$, ***, $^{\#\#\#}p<0.001$, significantly different from respective vehicle-treated groups by Dunnett's test.
doi:10.1371/journal.pone.0025788.g006

containing 0.2% Triton X-100 for 10 min (permeabilization). After blocking with 2% BSA in PBS, cells were incubated with primary antibody diluted with blocking buffer and then washed with PBS. Finally the cells were incubated with secondary antibodies and mounted using ProLong Gold antifade reagent with DAPI (Invitrogen). The immunoreactive cells were visualized using an LSM 700 Laser Scanning Microscope (Carl Zeiss, Jena, Germany) and a Biorevo BZ-9000 fluorescence microscope (Keyence, Osaka, Japan).

Quantitative real-time RT-PCR

Total RNA was isolated from cells using TRIZOL reagent (Invitrogen). Contaminating DNA was removed using the TURBO DNA-free kit (Ambion, Austin, TX), and cDNA was synthesized using ReverTra Ace-α (Toyobo, Osaka, Japan), according to the manufacturers' protocols. Real-time PCR was performed using the StepOnePlus system (Applied Biosystems) and SYBR green reagent (TAKARA, Shiga, Japan). The primers used are listed in Table S2 in the supporting information.

HiPS cell culture and differentiation into neuronal cells

HiPS cells, 253G4 [14] (passage 20–30) or hES cells, H9 were cultured on mitomycin C-treated mouse embryonic fibroblasts in primate ES medium (ReproCELL, Kanagawa, Japan) supplemented with bFGF (Wako Pure Chemicals, Osaka, Japan). To obtain cortical neurons derived from iPS cells, we partially modified a previous method [12,15]. For neural induction, partially dissociated iPS cell colonies, 40–100 μm in diameter, were selected with Cell Strainer (BD Falcon, BD Bioscience, Bedford, MA) and plated on poly-L-lysine (Sigma-Aldrich)/Laminin (BD Biosciences) (PLL/LM)-coated dishes (P1) in N2B27 neuronal differentiation medium [DMEM/F12 (Invitrogen), Neurobasal (Invitrogen), N2 (Invitrogen), B27 minus vitamin A (Invitrogen), L-Gln (Invitrogen)], supplemented with 100 ng/ml human recombinant Noggin (R&D Systems, Minneapolis, MN) and 1 μM SB431542 (Sigma-Aldrich) for 17 days. At day 10, primary colonies were split into small clumps using 200 U/ml collagenase with $CaCl_2$ and plated into PLL/Entactin-Collagen IV-Laminin (Millipore) (ECL)-coated dishes (P2). At day 17, P2 cells were dissociated using Accutase (Innovative Cell Technologies, San Diego, CA) and cultured on PLL/ECL-coated dishes (P3). Finally, at day 24, cells dissociated with Accutase were passed through a 40-μm cell strainer (BD Biosciences), counted, and cultured on PLL/LM/Fibronectin (Millipore)-coated 24-well plates at 2.5×10^4 cells/well in N2B27 medium supplemented with 10 ng/ml BDNF, GDNF, and NT-3 (R&D Systems). Medium changes for cell culture were carried out once every two or three days until day 52.

Aβ sandwich ELISA

At days 38, 45, and 52, two-day incubated conditioned media were collected from cultured neuronal cells and centrifuged at 4,000 *g* for 10 min. The resultant clear supernatants were subjected to sandwich ELISA (Wako) with a combination of monoclonal antibodies specific to the midportion of Aβ and specific to the C-terminal of Aβ40 or Aβ42, to determine the amounts of secreted Aβ, as described previously [20,28,30]. We also examined the inhibitory effect of each drug on Aβ production. All media were replaced with new media containing each drug and two-day conditioned media were analyzed as mentioned above.

Western blot analysis

Western blot analysis was performed as previously described with minor modification. In addition to conditioned media, cell lysates were also collected, extensively washed with PBS, and lysed

Table 1. Panel of Aβ monitoring systems.

Human sample	**Aβ40**	**Aβ42**	**Ref.**
Brain tissue [AD]	↑ (AD/NC)	↑ (AD/NC)	[39]
CSF [AD]	-	↓ (AD/NC)	[37]
	→ (AD/NC)	↓ (AD/NC)	[29]
Plasma [AD]	↑ (AD/NC)	→ (AD/NC)	[29]
iPS cell-derived neuronal cells	Measurable	Measurable	This report
Mouse model	**Aβ40**	**Aβ42**	**Ref.**
Brain [PDAPP]	↑ (Aging)	↑ (Aging)	[36]
Brain [APP23]	↑ (Tg/non-Tg)	↑ (Tg/non-Tg)	[27]
Brain [Tg2576]	↑ (Aging)	↑ (Aging)	[28]
	↑ (Tg/non-Tg)	↑ (Tg/non-Tg)	
CSF [Tg2576]	↓ (Aging)	↓ (Aging)	[28]
Plasma [Tg2576]	↓ (Aging)	↓ (Aging)	[28]
Cell line	**Aβ40**	**Aβ42**	**Ref.**
[APP_{NL}-H4]	Measurable	Measurable	[30]
[CHO-APP_{NL}/SH-SY5Y-APP]	Measurable	Measurable	[4]

AD, Alzheimer's disease; NC, normal control; Tg, transgenic mouse model.
doi:10.1371/journal.pone.0025788.t001

directly with 1× sample buffer (EzApply; ATTO, Tokyo, Japan). The media or cell lysates were separated by 5–20% gradient or 7.5% [FL-APP] or 10% [β-actin] sodium dodecyl sulfate-polyacrylamide gel electrophoresis (SDS-PAGE) and transferred to polyvinylidene difluoride membranes (Hybond-P; GE Healthcare, Buckinghamshire, UK). The blots were probed with an appropriate primary antibody, followed by HRP-conjugated anti-mouse or anti-rabbit IgG (GE Healthcare). The protein bands were visualized using an enhanced chemiluminescence (ECL) detection method (GE Healthcare), and band intensity was analyzed with a densitometer (LAS-4000; GE Healthcare), using the Science Laboratory 2001 Image Gauge software (Fujifilm, Tokyo, Japan). Immunoreactive protein content in each sample was calculated based on a standard curve constructed with each recombinant protein or one of the samples. Each set of experiments was repeated at least two times to confirm the results. The level of β-actin protein, measured by quantitative western blotting using β-actin antibody, was used as an extraction and loading control.

LDH assay

Cell toxicity assays were performed using a cytotoxicity detection kit (LDH, Roche, Mannheim, Germany) according to the manufacturer's protocol.

Statistical analysis

All data were expressed as mean ± SD. Comparisons of mean among more than three groups were done by one-way or two-way ANOVA, followed by *post-hoc* test (PRISM, GraphPad software). *P* values ≤0.05 indicated significant differences.

Supporting Information

Figure S1 Cholinergic neuronal marker-positive cells were observed in hiPS cell-derived neuronal cells. Expression levels of ChAT (A) and VAChT (B) were quantified by qPCR (n = 3) and normalized by that of GAPDH. "Fold expression" represents the ratio of expression on the given day compared to day 38. ChAT- (C) and VAChT (D)-positive cells were observed a little at day 52.
(TIF)

Figure S2 Percentages of the three isoforms of APP (APP770, APP751, and APP695) at 38, 45, and 52 days. Each column represents mean ± SD of 8 assays. $^{*}p<0.05$, $^{**}p<0.01$, $^{***}p<0.001$, Tukey's test.
(TIF)

Figure S3 New hsAPPα and sAPPβ antibodies specifically detect human sAPPα and sAPPβ by western blots, respectively. Human neuroglioma H4 cells overexpressing wild-type APP (APP_{WT}-H4 cells) were treated with α-secretase activator (12-*O*-tetradecanoylphorbol 13-acetate (TPA)), α-secretase inhibitor (TNF-α protease inhibitor-2 (TAPI-2)), or β-secretase inhibitor (see Protocol S1). Brain lysates of APP-knockout mice (APP-KO) were used as negative control. Immunoblots of conditioned media and supernatants of brain lysates were probed by anti-hsAPPα or anti-sAPPβ antibody. sAPPα or sAPPβ derived from both exogenous APP695 and endogenous APP770/751 are detected by each antibody. The increase in sAPPα by α-secretase activator and the reduction in sAPPα by α-secretase inhibitor effectively reached 434% and 50% of control (DMSO), respectively (upper panel). The decrease in sAPPβ by β-secretase inhibitor effectively reached 11% of control (lower panel). Neither sAPPα nor sAPPβ in the APP-KO brain was detected by anti-hsAPPα or anti-sAPPβ antibody, respectively. An asterisk indicates a non-specific band.
(TIF)

Figure S4 Immunocytochemical characterization of human ES cell (H9)-derived neuronal cells. (A) Time-dependent morphological changes of cells reseeded in a 24-well plate. Neuronal and glial cells were stained by anti-Tuj1 (left; red), anti-synapsin I (left; green), anti-MAP2 (right; red), and anti-GFAP (right; green) antibodies and DAPI (right; blue) at 38, 45, and 52 days. Scale bar, left; 20 μm, right; 50 μm. (B) ICC staining of Tbr1-, Ctip2-, Cux1- and Satb2-positive cells at day 52. (C–E) Neurotransmitter phenotypes at day 52. PAG (red)- and GAD (green)-positive (C), Glut1 (green)- and Tuj1 (red)-positive (D), and GABA (green)- and Tuj1 (red)-positive cells (E). Blue, DAPI. Scale bar, 50 μm.
(TIF)

Figure S5 Aβ production was modulated by several drugs in human ES cell-derived neuronal cells. β-Secretase inhibitor (BSI) (A, B), γ-secretase inhibitor (GSI) (C, D), and NSAID (E, F) were added into hES cell-derived neuronal cell cultures at day 36 (dotted line) and 50 (bold line), and two days later amounts of Aβ40 and Aβ42 secreted into the conditioned media were measured. The ratios Aβ40/FL-APP and Aβ42/FL-APP are expressed as percentages of the vehicle-treated group at day 52 and represent mean ± SD of 3 assays. *, $^{\#}p<0.05$, **, $^{\#\#}p<0.01$, ***, $^{\#\#\#}p<0.001$, significantly different from respective vehicle-treated groups by Dunnett's test.
(TIF)

Figure S6 Expression levels of reprogramming factors of iPS cells in neural differentiation. Total and transgene (Tg) expression levels of Sox2, Oct3/4 and Klf4 were measured by qPCR. Bold and dotted lines represent total and transgene expressions, respectively. "Fold expression" represents the ratio of the expression level compared to the total expression level at day 0 (iPS cells).
(TIF)

Figure S7 Aβ production was modulated by GSI in human iPS cell (201B7)-derived neuronal cells. γ-Secretase inhibitor (GSI) was added into the hiPS cell line, 201B7-derived neuronal cell cultures at day 36 (dotted line) and 50 (bold line), and two days later amounts of Aβ40 (A) and Aβ42 (B) secreted into the conditioned media were measured. The ratios Aβ40/FL-APP and Aβ42/FL-APP are expressed as percentages of the vehicle-treated group at day 52 and represent mean ± SD of 3 assays.
(TIF)

Protocol S1 Sampling method for checking antibody specificity.
(PDF)

Table S1 Effects of secretion inhibitors on cell viability measured by LDH assay at day 52.
(DOCX)

Table S2 qPCR primers.
(DOCX)

Acknowledgments

We would like to express our sincere gratitude to all our coworkers and collaborators, especially to K. Watanabe (RIKEN Brain Science Institute & Nagasaki University) for technical assistance and to K. Murai (CiRA) for editing manuscript.

Author Contributions

Conceived and designed the experiments: NI HI NY MA. Performed the experiments: NY MA NI. Analyzed the data: NY MA NI HI. Contributed reagents/materials/analysis tools: SK KT IA HH TK KM TCS TN TA SY. Wrote the paper: NY MA SY NI HI.

References

1. Selkoe DJ (2002) Alzheimer's disease is a synaptic failure. Science 298: 789–791.
2. Iwata N, Higuchi M, Saido TC (2005) Metabolism of amyloid-β peptide and Alzheimer's disease. Pharmacol Ther 108: 129–148.
3. Kukar TL, Ladd TB, Bann MA, Fraering PC, Narlawar R, et al. (2008) Substrate-targeting γ-secretase modulators. Nature 453: 925–929.
4. Kounnas MZ, Danks AM, Cheng S, Tyree C, Ackerman E, et al. (2010) Modulation of γ-secretase reduces β-amyloid deposition in a transgenic mouse model of Alzheimer's disease. Neuron 67: 769–780.
5. Takahashi K, Tanabe K, Ohnuki M, Narita M, Ichisaka T, et al. (2007) Induction of pluripotent stem cells from adult human fibroblasts by defined factors. Cell 131: 861–872.
6. Yu J, Vodyanik MA, Smuga-Otto K, Antosiewicz-Bourget J, Frane JL, et al. (2007) Induced pluripotent stem cell lines derived from human somatic cells. Science 318: 1917–1920.
7. Watanabe K, Kamiya D, Nishiyama A, Katayama T, Nozaki S, et al. (2005) Directed differentiation of telencephalic precursors from embryonic stem cells. Nat Neurosci 8: 288–296.
8. Gaspard N, Bouschet T, Hourez R, Dimidschstein J, Naeije G, et al. (2008) An intrinsic mechanism of corticogenesis from embryonic stem cells. Nature 455: 351–357.
9. Eiraku M, Watanabe K, Matsuo-Takasaki M, Kawada M, Yonemura S, et al. (2008) Self-organized formation of polarized cortical tissues from ESCs and its active manipulation by extrinsic signals. Cell Stem Cell 3: 519–532.
10. Li XJ, Zhang X, Johnson MA, Wang ZB, Lavaute T, et al. (2009) Coordination of sonic hedgehog and Wnt signaling determines ventral and dorsal telencephalic neuron types from human embryonic stem cells. Development 136: 4055–4063.
11. Zeng H, Guo M, Martins-Taylor K, Wang X, Zhang Z, et al. (2010) Specification of region-specific neurons including forebrain glutamatergic neurons from human induced pluripotent stem cells. PLoS One 5: e11853.
12. Chambers SM, Fasano CA, Papapetrou EP, Tomishima M, Sadelain M, et al. (2009) Highly efficient neural conversion of human ES and iPS cells by dual inhibition of SMAD signaling. Nat Biotechnol 27: 275–280.
13. Braak H, Braak E (1991) Neuropathological stageing of Alzheimer-related changes. Acta Neuropathol 82: 239–259.
14. Nakagawa M, Koyanagi M, Tanabe K, Takahashi K, Ichisaka T, et al. (2008) Generation of induced pluripotent stem cells without Myc from mouse and human fibroblasts. Nat Biotechnol 26: 101–106.
15. Wada T, Honda M, Minami I, Tooi N, Amagai Y, et al. (2009) Highly efficient differentiation and enrichment of spinal motor neurons derived from human and monkey embryonic stem cells. PLoS One 4: e6722.
16. Saito T, Hanai S, Takashima S, Nakagawa E, Okazaki S, et al. (2011) Neocortical layer formation of human developing brains and lissencephalies: consideration of layer-specific marker expression. Cereb Cortex 21: 588–596.
17. Kim JE, O'Sullivan ML, Sanchez CA, Hwang M, Israel MA, et al. (2011) Investigating synapse formation and function using human pluripotent stem cell-derived neurons. Proc Natl Acad Sci U S A 108: 3005–3010.
18. Akiyama H, Kaneko T, Mizuno N, McGeer PL (1990) Distribution of phosphate-activated glutaminase in the human cerebral cortex. J Comp Neurol 297: 239–252.
19. Blennow K, de Leon MJ, Zetterberg H (2006) Alzheimer's disease. Lancet 368: 387–403.
20. Kitazume S, Tachida Y, Kato M, Yamaguchi Y, Honda T, et al. (2010) Brain endothelial cells produce amyloid β from amyloid precursor protein 770 and preferentially secrete the O-glycosylated form. J Biol Chem 285: 40097–40103.
21. Yang LB, Lindholm K, Yan R, Citron M, Xia W, et al. (2003) Elevated β-secretase expression and enzymatic activity detected in sporadic Alzheimer disease. Nat Med 9: 3–4.
22. O'Connor T, Sadleir KR, Maus E, Velliquette RA, Zhao J, et al. (2008) Phosphorylation of the translation initiation factor eIF2α increases BACE1 levels and promotes amyloidogenesis. Neuron 60: 988–1009.
23. Parks AL, Curtis D (2007) Presenilin diversifies its portfolio. Trends Genet 23: 140–150.
24. Serneels L, Van Biervliet J, Craessaerts K, Dejaegere T, Horré K, et al. (2009) γ-Secretase heterogeneity in the Aph1 subunit: relevance for Alzheimer's disease. Science 324: 639–642.
25. McGowan E, Pickford F, Kim J, Onstead L, Eriksen J, et al. (2005) Aβ42 is essential for parenchymal and vascular amyloid deposition in mice. Neuron 47: 191–199.
26. Ono K, Condron MM, Ho L, Wang J, Zhao W, et al. (2008) Effects of grape seed-derived polyphenols on amyloid β-protein self-assembly and cytotoxicity. J Biol Chem 283: 32176–32187.
27. Hsiao K, Chapman P, Nilsen S, Eckman C, Harigaya Y, et al. (1996) Correlative memory deficits, Aβ elevation, and amyloid plaques in transgenic mice. Science 274: 99–102.
28. Kawarabayashi T, Younkin LH, Saido TC, Shoji M, Ashe KH, et al. (2001) Age-dependent changes in brain, CSF, and plasma amyloid β protein in the Tg2576 transgenic mouse model of Alzheimer's disease. J Neurosci 21: 372–381.
29. Mehta PD, Pirttilä T, Mehta SP, Sersen EA, Aisen PS, et al. (2000) Plasma and cerebrospinal fluid levels of amyloid β proteins 1-40 and 1-42 in Alzheimer disease. Arch Neurol 57: 100–105.
30. Asai M, Iwata N, Tomita T, Iwatsubo T, Ishiura S, et al. (2010) Efficient four-drug cocktail therapy targeting amyloid-β peptide for Alzheimer's disease. J Neurosci Res 88: 3588–3597.
31. Stachel SJ, Coburn CA, Steele TG, Jones KG, Loutzenhiser EF, et al. (2004) Structure-based design of potent and selective cell-permeable inhibitors of human β-secretase (BACE-1). J Med Chem 47: 6447–6450.
32. Seiffert D, Bradley JD, Rominger CM, Rominger DH, Yang F, et al. (2000) Presenilin-1 and -2 are molecular targets for γ-secretase inhibitors. J Biol Chem 275: 34086–34091.
33. Weggen S, Eriksen JL, Das P, Sagi SA, Wang R, et al. (2001) A subset of NSAIDs lower amyloidogenic Aβ42 independently of cyclooxygenase activity. Nature 414: 212–216.
34. Eriksen JL, Sagi SA, Smith TE, Weggen S, Das P, et al. (2003) NSAIDs and enantiomers of flurbiprofen target γ-secretase and lower Aβ 42 in vivo. J Clin Invest 112: 440–449.
35. Burton CR, Meredith JE, Barten DM, Goldstein ME, Krause CM, et al. (2008) The amyloid-β rise and γ-secretase inhibitor potency depend on the level of substrate expression. J Biol Chem 283: 22992–23003.
36. Games D, Adams D, Alessandrini R, Barbour R, Berthelette P, et al. (1995) Alzheimer-type neuropathology in transgenic mice overexpressing V717F β-amyloid precursor protein. Nature 373: 523–527.
37. De Meyer G, Shapiro F, Vanderstichele H, Vanmechelen E, Engelborghs S, et al. (2010) Diagnosis-independent Alzheimer disease biomarker signature in cognitively normal elderly people. Arch Neurol 67: 949–956.
38. Inoue H, Yamanaka S (2011) The use of induced pluripotent stem cells in drug development. Clin Pharmacol Ther 89: 655–661.
39. Iwatsubo T, Saido TC, Mann DM, Lee VM, Trojanowski JQ (1996) Full-length amyloid-β (1-42(43)) and amino-terminally modified and truncated amyloid-β 42(43) deposit in diffuse plaques. Am J Pathol 149: 1823–1830.
40. Johnson MA, Weick JP, Pearce RA, Zhang SC (2007) Functional neural development from human embryonic stem cells: accelerated synaptic activity via astrocyte coculture. J Neurosci 27: 3069–3077.
41. Lazarov O, Lee M, Peterson DA, Sisodia SS (2002) Evidence that synaptically released β-amyloid accumulates as extracellular deposits in the hippocampus of transgenic mice. J Neurosci 22: 9785–9793.
42. Soba P, Eggert S, Wagner K, Zentgraf H, Siehl K, et al. (2005) Homo- and heterodimerization of APP family members promotes intercellular adhesion. EMBO J 24: 3624–3634.
43. Woo SM, Kim J, Han HW, Chae JI, Son MY, et al. (2009) Notch signaling is required for maintaining stem-cell features of neuroprogenitor cells derived from human embryonic stem cells. BMC Neurosci 10: 97.
44. Mangialasche F, Solomon A, Winblad B, Mecocci P, Kivipelto M (2010) Alzheimer's disease: clinical trials and drug development. Lancet Neurol 9: 702–716.
45. Qiang L, Fujita R, Yamashita T, Angulo S, Rhinn H, et al. (2011) Directed conversion of Alzheimer's disease patient skin fibroblasts into functional neurons. Cell 146: 359–371.
46. Kaneko T, Urade Y, Watanabe Y, Mizuno N (1987) Production, characterization, and immunohistochemical application of monoclonal antibodies to glutaminase purified from rat brain. J Neurosci 7: 302–309.
47. Saido TC, Nagao S, Shiramine M, Tsukaguchi M, Sorimachi H, et al. (1992) Autolytic transition of mu-calpain upon activation as resolved by antibodies distinguishing between the pre- and post-autolysis forms. J Biochem 111: 81–86.

Biochemical and Biophysical Research Communications 417 (2012) 116–121

Contents lists available at SciVerse ScienceDirect

Biochemical and Biophysical Research Communications

journal homepage: www.elsevier.com/locate/ybbrc

Epitope mapping of antibodies against TDP-43 and detection of protease-resistant fragments of pathological TDP-43 in amyotrophic lateral sclerosis and frontotemporal lobar degeneration

Hiroshi Tsuji [a,b], Takashi Nonaka [a], Makiko Yamashita [a], Masami Masuda-Suzukake [a], Fuyuki Kametani [a], Haruhiko Akiyama [c], David M.A. Mann [d], Akira Tamaoka [b], Masato Hasegawa [a,*]

[a] Department of Neuropathology and Cell Biology, Tokyo Metropolitan Institute of Medical Science, 2-1-6 Kamikitazawa, Setagaya-ku, Tokyo 156-8506, Japan
[b] Department of Neurology, Graduate School of Comprehensive Human Sciences, University of Tsukuba, 1-1-1 Tenodai, Tsukuba-City, Ibaraki 305-8576, Japan
[c] Dementia Research Project, Tokyo Metropolitan Institute of Medical Science, 2-1-6 Kamikitazawa, Setagaya-ku, Tokyo 156-0057, Japan
[d] Mental Health and Neurodegeneration Research Group, Greater Manchester Neuroscience Centre, University of Manchester, Hope Hospital, Salford M6 8HD, UK

ARTICLE INFO

Article history:
Received 8 November 2011
Available online 22 November 2011

Keywords:
Aggregation
Tau
Alpha-synuclein
ALS
FTLD

ABSTRACT

TAR DNA-binding protein of 43 kDa (TDP-43) is the major component of the intracellular inclusions in amyotrophic lateral sclerosis (ALS) and frontotemporal lobar degeneration (FTLD). Here, we show that both monoclonal (60019-2-Ig) and polyclonal (10782-2-AP) anti-TDP-43 antibodies recognize amino acids 203–209 of human TDP-43. The monoclonal antibody labeled human TDP-43 by recognizing Glu204, Asp205 and Arg208, but failed to react with mouse TDP-43. The antibodies stained the abnormally phosphorylated C-terminal fragments of 24–26 kDa in addition to normal TDP-43 in ALS and FTLD brains. Immunoblot analysis after protease treatment demonstrated that the epitope of the antibodies (residues 203–209) constitutes part of the protease-resistant domain of TDP-43 aggregates which determine a common characteristic of the pathological TDP-43 in both ALS and FTLD-TDP. The antibodies and methods used in this study will be useful for the characterization of abnormal TDP-43 in human materials, as well as in vitro and animal models for TDP-43 proteinopathies.

1. Introduction

TDP-43 is a nuclear ribonucleoprotein implicated in exon splicing, gene transcription, regulation of mRNA stability, mRNA biosynthesis, and formation of nuclear bodies [1–5]. It has been identified as the major component of the ubiquitin-positive tau-negative intracytoplasmic inclusions in frontotemporal lobar degeneration (FTLD), amyotrophic lateral sclerosis (ALS) [6,7] and other neurodegenerative disorders [8–12]. Identification of mutations in familial and sporadic ALS and FTLD cases demonstrated a direct link between the genetic lesion and development of TDP-43 pathology [13–16]. Immunohistochemical studies using anti-TDP-43 antibodies revealed that TDP-43 translocates from its normal nuclear localization into the cytoplasm in these disorders. Furthermore, biochemical analysis detected abnormally phosphorylated TDP-43 of 45 kDa, high-molecular-weight smearing and C-terminal fragments of approximately 25 kDa, as well as normal TDP-43 of 43 kDa in the detergent-insoluble, urea-soluble fraction from affected brains. The antibodies generated by immunizing C-terminal phosphopeptides of TDP-43, such as pS409/410 and pS403/404, strongly stain abnormal neuronal cytoplasmic and dendritic inclusions in FTLD, and skein-like and glial cytoplasmic inclusions in ALS spinal cord, with no nuclear staining, and thus permit easier and more sensitive detection of abnormal TDP-43 accumulations in neuropathological examination [17]. Immunoblotting of the Sarkosyl-insoluble fractions from FTLD and ALS cases using these phosphospecific antibodies clearly demonstrated that hyperphosphorylated full-length TDP-43 of 45 kDa, smearing substances and fragments at 18–26 kDa are the major species of TDP-43 accumulated in FTLD and ALS, and the band patterns of the C-terminal fragments of phosphorylated TDP-43 correspond to the neuropathological subtypes.

Anti-TDP-43 monoclonal antibody (mAb) (60019-2-Ig; Proteintech Group Inc., Chicago, IL) and polyclonal antibody (pAb) (10782-2-AP; Proteintech Group Inc., Chicago, IL) are widely used for the investigation of TDP-43 pathology [6,7,9,18–21]. According to the manufacturer's specifications, anti-TDP-43 mAb and pAb were generated against the N-terminal 260 amino acids (aa) of the protein, but the precise epitope has not yet been identified. Another mouse monoclonal antibody against TDP-43 (2E2-D3; Abnova Corporation, Taipei, Taiwan) is also commercially available; it recognizes residues 205–222 of human TDP-43, but does not recognize mouse or rat TDP-43 [22].

* Corresponding author. Fax: +81 3 6834 2349.
E-mail address: hasegawa-ms@igakuken.or.jp (M. Hasegawa).

0006-291X/$ - see front matter © 2011 Elsevier Inc. All rights reserved.
doi:10.1016/j.bbrc.2011.11.066

In this study, we mapped the epitope for anti-TDP-43 mAb and pAb (Proteintech Group Inc.). We also showed that anti-TDP-43 mAb recognizes human TDP-43, but not mouse TDP-43. Using these antibodies, we investigated the abnormal forms of TDP-43 from ALS and FTLD brains, and found that the antibodies recognized the amino-terminus of the TDP-43 C-terminal fragments of 24–26 kDa. Immunoblot analysis of Sarkosyl-insoluble fractions after treatment of proteases also demonstrated that the epitope is apparently resistant to trypsin and chymotrypsin in the abnormal TDP-43, suggesting that the epitope region is important for the formation of the pathological structure of TDP-43 in ALS and FTLD.

2. Materials and methods

2.1. Construction of plasmids

GFP-tagged TDP-43 C-terminal or N-terminal fragments were constructed as described [23] by amplifying a cDNA encoding full-length TDP-43 by means of PCR and inserting the fragment into the pEGFP-C1 vector (Clontech). To investigate the specificity of TDP-43 mAb for human TDP-43, site-directed mutagenesis of GFP-tagged full-length TDP-43 was carried out to substitute Glu204 to Ala (E204A), Asp205 to Glu (D205E), Arg208 to Gln (R208Q), Glu209 to Gln (E209Q), Ser212 to Cys (S212C), Asp216 to Glu (D216E), and Met218 to Val (M218V), using a site-directed mutagenesis kit (Strategene)(Fig. 4). All constructs were verified by DNA sequencing.

2.2. Antibodies

TDP-43 polyclonal antibody, 10782-2-AP, and TDP-43 monoclonal antibody, 60019-2-Ig, were purchased from Proteintech Group Inc. Anti-GFP monoclonal antibody was purchased from MBL (Nagoya, Japan). A polyclonal antibody specific for phosphorylated TDP-43 (pS409/410) was prepared as described [17].

2.3. Cell culture and expression of plasmids

Human neuroblastoma cell line SH-SY5Y and mouse neuroblastoma cell line Neuro 2a were maintained in appropriate medium as described previously [24,25]. Cells were then transfected with expression plasmids using FuGENE6 (Roche) according to the manufacturer's instructions.

2.4. Immunoblotting

Expressed proteins in cell lysates were separated by 10% SDS–PAGE and transferred onto polyvinylidene difluoride membrane (Millipore, Bedford, MA). After blocking with 3% gelatin, membranes were incubated overnight with primary antibodies (1:1000) at room temperature. After incubation with an appropriate biotinylated secondary antibody, labeling was detected using the ABC system (Vector Lab., Burlingame, CA) coupled with a diaminobenzidine (DAB) reaction intensified with nickel chloride.

2.5. Analysis of abnormal TDP-43 in ALS and FTLD-TDP brain

Brains from two cases with Alzheimer's disease (AD), two with ALS, two with FTLD-TDP (type A), two with FTLD-TDP (type B) and two with FTLD-TDP (type C) were employed in this study. The two AD cases had no TDP-43 pathology. The age, sex, brain weight, and diagnosis are given in Table 1. Sarkosyl-insoluble, urea-soluble fractions were extracted from these brains as previously described [6,9]. The samples were loaded onto 15% polyacrylamide gel and transferred onto a membrane. The membrane was cut in the center of the loaded lane, and the same samples were reacted separately with anti-TDP-43 Abs and pS409/410 as described above.

Table 1
Description of subjects.

Case No.	Diagnosis	Age (years)	Sex	BW (g)
1	AD	65	F	1165
2	AD	70	F	1126
3	ALS	62	M	1230
4	ALS	42	F	1140
5	FTLD-TDP (type A)	71	F	863
6	FTLD-TDP (type A)	66	F	1100
7	FTLD-TDP (type B)	45	M	1260
8	FTLD-TDP (type B)	67	M	1280
9	FTLD-TDP (type C)	67	M	na
10	FTLD-TDP (type C)	59	M	na

BW, brain weight; AD, Alzheimer's disease; ALS, amyotrophic lateral sclerosis; FTLD-TDP, frontotemporal lobar degeneration with TDP-43 pathology; na, not available.

2.6. Protease treatment of TDP-43

Sarkosyl-insoluble fractions extracted from neocortical regions of the brains were treated with trypsin (at a final concentration of 100 μg/ml, Promega, Madison, USA) or chymotrypsin (at a concentration of 10 μg/ml, Sigma–Aldrich, St. Louis, USA) at 37 °C for 30 min. The reaction was stopped by boiling for 5 min. After centrifuging at 15,000 rpm for 1 min, the samples were analyzed by immunoblotting with anti-TDP-43 pAb and mAb as described above.

3. Results

3.1. Epitope mapping of anti-TDP-43 antibody

Our previous study showed that both TDP-43 mAb and pAb reacted with GFP-tagged TDP-43 C-terminal fragment (GFP-TDP 162–414), but failed to detect GFP-TDP 218–414 [23]. To map the epitope of these antibodies, we expressed a series of GFP-tagged human TDP-43 C-terminal fragments (Fig. 1A) in SH-SY5Y cells and immunoblotted them with the antibodies. Both anti-TDP-43 pAb and mAb detected endogenous human TDP-43 of 43 kDa and exogenous GFP-tagged full-length, 171–414, 181–414, 191–414 and 201–414 TDP-43. However, both antibodies failed to detect 211–414 (Fig. 1A). These results suggest that the epitopes of these antibodies are located within residues 201–210.

To narrow down the epitope structure further, another series of GFP-tagged C-terminal fragments of TDP-43 was expressed in SH-SY5Y cells (Fig. 1B) and tested. Both antibodies reacted with GFP-TDP 203–414, but failed to recognize GFP-TDP 204–414, 205–414 and 207–414 (Fig. 1B), demonstrating that Thr203 forms the N-terminal border of the epitope for both antibodies.

To determine the C-terminus of the epitope, a series of GFP-tagged N-terminal fragments of TDP-43 was expressed and immunoblotted with these antibodies (Fig 1C). Anti-TDP-43 pAb reacted with all of the N-terminal fragments tested, although it stained the 1-212 fragment most strongly. This suggests that one of the pAb epitopes is located at the N-terminal region of TDP-43, in addition to the central epitope. Anti-TDP-43 mAb strongly stained GFP-TDP 1-212, moderately stained GFP-TDP 1-210, and barely stained GFP-TDP 1-209, while it failed to react with GFP 1-208 and 1-207 (Fig. 1C), indicating that Glu209 forms the C-terminus of the epitope for anti-TDP-43 mAb. Thus, anti-TDP-43 mAb recognizes residues 203–209 of human TDP-43.

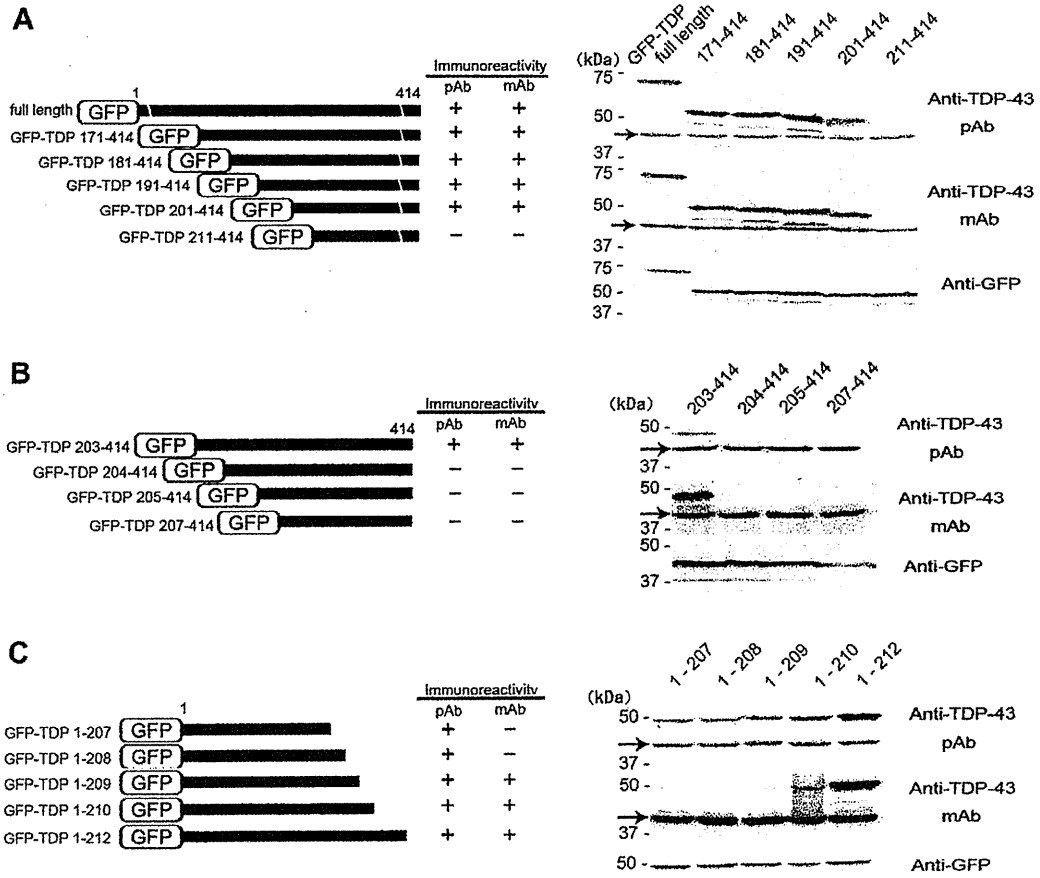

Fig. 1. Epitope mapping of anti-TDP-43 polyclonal and monoclonal antibodies. (A) Schematic diagram of GFP-tagged full-length TDP-43 (GFP-TDP) and the C-terminal fragments. Immunoblot analyses of GFP-TDP and the C-terminal fragments in SH-SY5Y cells. Both mAb and pAb reacted with GFP-TDP and the C-terminal fragments, except for 211–414. The anti-GFP antibody recognizes all the proteins expressed. (B) Further epitope mapping of anti-TDP-43 antibodies. Immunoblot analyses of the GFP tagged C-terminal fragments of TDP-43. Both mAb and pAb reacted with 203–414, but failed to recognize 204–414, 205–414, and 207–414. The anti-GFP antibody recognizes all of the fragments. (C) Epitope mapping of the C-terminus recognized by anti-TDP-43 polyclonal and monoclonal antibodies. Immunoblot analyses of GFP-TDP and N-terminal fragments in SH-SY5Y cells. Anti-TDP-43 pAb reacted with all of the N-terminal fragments, although it stained 1-212 fragment most strongly. In contrast, anti-TDP-43 mAb strongly stained GFP-TDP 1-212, moderately stained GFP-TDP 1-210, and barely stained GFP-TDP 1-209, while it failed to react with GFP 1-208 and 1-207. The anti-GFP antibody recognized all of the fragments equally. The arrows indicate endogenous TDP-43 in SH-SY5Y cells.

3.2. Amino acid sequence differences between human and mouse TDP-43

The anti-TDP-43 mAb reacted with endogenous TDP-43 of human neuroblastoma SH-SY5Y cells, but not with TDP-43 of mouse neuroblastoma Neuro2a cells (Fig. 1B, 1C, 2B). Similarly, the mAb recognized TDP-43 in human brain extract, but failed to detect TDP-43 in mouse brain extract, suggesting that the mAb does not recognize mouse TDP-43 (data not shown). The absence of reactivity with mouse TDP-43 is explained by the sequence differences around the epitope between human and mouse TDP-43 (Fig. 2A). Each different amino acid of human TDP-43 was substituted to that of mouse TDP-43. The mutated proteins were expressed in Neuro2a cells and immunoreactivity with anti-TDP-43 mAb was examined. Substitution of D216 to E and M218 to V did not affect the immunoreactivity (Fig. 2B), whereas substitutions of E204 to A, D205 to E, and R208 to Q abolished the immunoreactivity of anti-TDP-43 mAb, indicating that these residues are necessary for recognition by the mAb. Anti-TDP-43 pAb reacted with these mutants, although a marked decrease in immunoreactivity was observed in the cases of E204A, D205A, R208Q, and S212C.

3.3. Biochemical analysis of abnormal TDP-43 in ALS and FTLD brains with anti-TDP-43 mAb

On immunoblots of Sarkosyl-insoluble fractions extracted from the brain of patients with ALS and FTLD-TDP (type A), the anti-TDP-43 mAb detected phosphorylated full-length TDP-43 at 45 kDa, two bands around 25 kDa and high-molecular-weight smears, in addition to the normal TDP-43 band at 43 kDa, which can also be detected in control cases. Immunoblot analysis of the split membrane with a phosphorylation-dependent anti-TDP-43 antibody pS409/410 revealed that the two bands around 25 kDa stained with the mAb corresponded to the C-terminal fragments of 24 and 26 kDa recognized by pS409/410 (Fig. 3)[17]. These results demonstrated that these 24 and 26 kDa C-terminal fragments contain the epitope of the mAb, residues 203–209, and that the cleavage sites of these C-terminal fragments are located at the N-terminal side of Thr203.

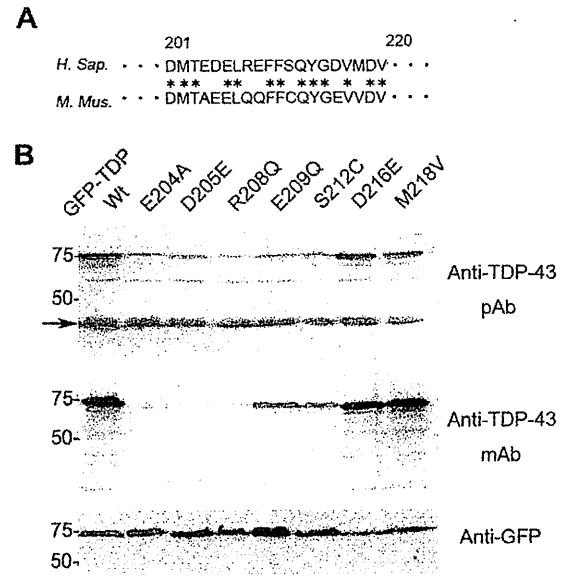

Fig. 2. Alignment of human and mouse TDP-43 (A) and immunoblot analyses of mutated TDP-43 with anti-TDP-43 antibodies. (A) The amino acid sequences of human (upper) and mouse (lower) TDP-43 around the epitope of anti-TDP-43 mAb. The asterisks show identical amino acids. (B) Immunoblot analyses of GFP-TDP wild type (Wt) and GFP-TDP mutants expressed in Neuro2a cells. Substitution of D216 to E and M218 to V did not affect the immunoreactivity, whereas substitutions of E204 to A, D205 to E, and R208 to Q, abolished the immunoreactivity of anti-TDP-43 mAb. Anti-TDP-43 pAb reacted with all these mutants, although markedly decreased immunoreactivities were observed in E204A, D205A, R208Q, and S212C. The arrows indicated endogenous TDP-43 in Neuro2A cells. Note that endogenous mouse TDP-43 in Neuro 2a cells was not recognized by anti-TDP-43 mAb.

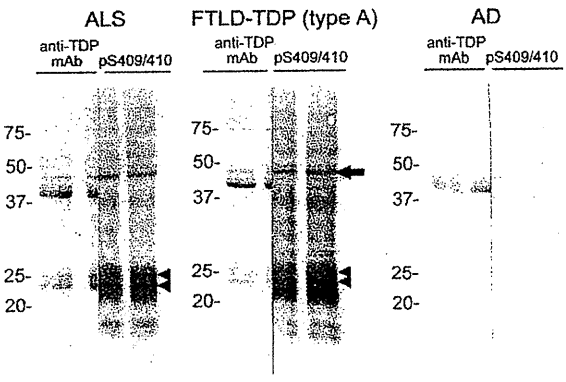

Fig. 3. Immunoblot analyses of Sarkosyl-insoluble fractions from ALS, FTLD-TDP (type A), and AD brains with anti-TDP-43 monoclonal antibody and phosphorylation-dependent anti-TDP-43 antibody, pS409/410. With pS409/410, fragments of approximately 45 kDa and 18–26 kDa, as well as smearing, were detected. The banding pattern of 18–26 kDa fragments showed three major bands at 23, 24, and 26 kDa, and 2 minor bands at 18 and 19 kDa, with the 24 kDa band being the most intense. In addition to the normal full-length TDP-43 at 43 kDa, anti-TDP-43 mAb labeled phosphorylated full-length TDP-43 at 45 kDa, high-molecular-weight smears and two bands at 26 kDa and 24 kDa (arrowheads), which were not seen in the AD case. The two bands corresponded to the major 26 and 24 kDa bands were detected with pS409/410.

3.4. The epitope of these TDP-43 antibodies constitute part of protease-resistant core domain of TDP-43 in ALS and FTLD brains

In order to characterize the epitope further, we treated the Sarkosyl-insoluble fractions extracted from brains of patients with proteases and analyzed them with these antibodies. Without protease treatment, both antibodies strongly stained normal full-length TDP-43 of 43 kDa in all cases examined including AD cases which were without TDP-43 pathology. In ALS and FTLD-TDP cases, phosphorylated full-length TDP-43 of 45 kDa (Fig 4A, arrows) and the ~25 kDa fragments (Fig 4A, arrow heads) were detected with these antibodies. After trypsin treatment, the full-length band of TDP-43 was disappeared and the protease-resistant fragments around 25 kDa (Fig 4B, white arrows) and smearing substances appeared in the ALS and FTLD-TDP cases. Similarly, after chymotrypsin treatment, protease-resistant triplet bands of 16, 20 and 25 kDa (Fig 4C, white arrow heads) and smearing substances were clearly detected in ALS and FTLD-TDP-cases with the mAb, while no such bands were seen in AD cases. On blot with the pAb, multiple bands were detected in addition to the triplet, and some of these bands were also detected in AD cases, suggesting that the pAb stained some normal fragments in addition to the abnormal TDP-43 bands. In the cases examined, apparent difference was not detected in these trypsin-resistant and chymotrypsin-resistant bands detected among the clinicopathological phenotypes of the diseases. By proteinase K treatment, immunoreactivities with these antibodies were completely abolished (data not shown), suggesting that the epitope is not entirely resistant to any proteases. However, it is obvious that the epitope of the TDP-43 deposited in the patients is fairly protease-resistant compared to the normal protein. These results indicate that the epitope of the mAb (residues 203–209 of TDP-43) constitute part of the protease-resistant domain of TDP-43 which determine a common characteristic of the abnormal TDP-43 in both ALS and FTLD-TDP.

4. Discussion

This is the first analysis of the epitopes of Proteintech's anti-TDP-43 polyclonal and monoclonal antibodies, which have often been used to research TDP-43 proteinopathies since 2006 [6,7]. We demonstrated that anti-TDP-43 mAb specifically recognizes residues 203–209 of human TDP-43, which form a part of the second RNA-recognition motif (RRM2, residues 193–257) of normal TDP-43 [26], but constitute part of the protease-resistant core domain of TDP-43 aggregates that determine the common characteristic of abnormal TDP-43 in ALS and FTLD-TDP-43.

RRM2 is a functional domain with distinct RNA/DNA binding characteristics. The anti-TDP-43 mAb recognized human TDP-43, but not mouse TDP-43. Site-directed mutagenesis and subsequent immunoblot analysis revealed that Glu204, Asp205 and Arg208 residues in human TDP-43 are important for the specific recognition by the mAb (Fig. 2). In fact, human TDP-43 shares 98.5% homology with mouse TDP-43 at the amino acid level, but the RRM2 domain has only 66% homology.

We also showed that one of the major epitopes of the pAb is located in almost the same region at that of the mAb (Fig. 1), although the pAb also recognizes the N-terminal region of TDP-43. Recently, TDP-43 transgenic mice overexpressing human TDP-43 have been produced as animal models of TDP-43 proteinopathy [27]. However, abnormal TDP-43 pathologies in these mice are very rare, so new transgenic or other animal models that develop abundant TDP-43 pathology are still required. Since the TDP-43 mAb recognizes human TDP-43, but not mouse TDP-43, it will be a useful reagent for the characterization of mouse lines transgenic for human TDP-43, together with phosphorylation-dependent antibodies.

Biochemical analyses of TDP-43 proteinopathies have demonstrated that abnormally phosphorylated full-length and C-terminal fragments of TDP-43 are the major species in the inclusions. The band patterns of the C-terminal fragments at 18–26 kDa are closely correlated with the clinicopathological subtypes of TDP-43 proteinopathies [17]. In addition, most of the pathogenic mutations

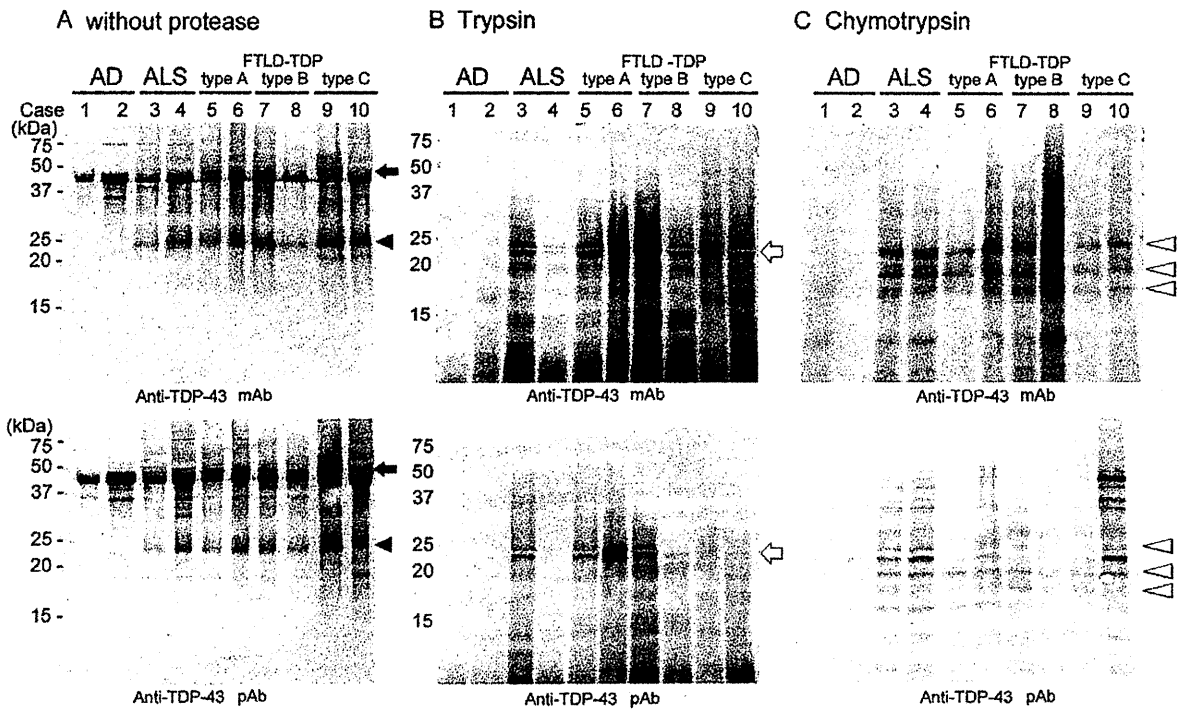

Fig. 4. Immunoblot analysis of Sarkosyl-insoluble fractions from AD and TDP-43 proteinopathies before and after protease treatment. (A) Without protease treatment, normal TDP-43 of 43 kDa was detected with these antibodies in all cases examined. In the ALS and FTLD-TDP cases, phosphorylated full-length TDP-43 of 45 kDa (arrows), high-molecular-weight smears, and the 24–26 kDa fragments (arrow heads) were detected in addition to the normal TDP-43. (B) Upon trypsin treatment, full-length TDP-43 disappeared, and the protease-resistant ~25 kDa fragments (white arrows) and smears appeared in ALS and FTLD-TDP cases, but not in AD cases. (C) After chymotrypsin treatment, triplet bands (white arrowheads) were detected in ALS and FTLD-TDP cases with the mAb and multiple bands were detected with pAb, whereas such immunoreactivities were hardly detected in AD cases.

are found in the C-terminal half of the TDP-43 [13–16]. Therefore, misfolding or structural alteration of the C-terminal half of TDP-43 seems to be the key to the pathogenesis of TDP-43 proteinopathies. By mass spectrometric analysis of the 23 kDa band in Sarkosyl-insoluble fraction from FTLD-TDP (type A), we identified the cleavage site as the N-terminus of Asp219 [23]. Another group reported cleavage at Asp208, based on N-terminal sequencing of urea extracts of FTLD-TDP brain [28]. However, the cleavage sites of the other major C-terminal fragments of 24 and 26 kDa have not been determined yet. In this study, we showed that the pathological TDP-43 C-terminal fragments of 24 and 26 kDa in ALS and FTLD-TDP type A contain the epitope of anti-TDP-43 mAb, residues 203–209, by comparing the immunoblotting results with those using pS409/410 (Fig. 3). This result suggests that the cleavage sites of pathological TDP-43 C-terminal fragments in ALS and FTLD-TDP are located at the N-terminal side of Thr203. Although the mechanisms of generation of the C-terminal fragments are still controversial, the presence of multiple cleavage sites suggests that cleavage may occur after the aggregation or assembly of TDP-43.

Structural or conformational changes in the proteins are thought to be the most important in protein aggregation in these neurodegenerative diseases. To analyze the conformational change in the epitope of TDP-43 from normal to the abnormal states further, we treated the Sarkosyl-insoluble TDP-43 with trypsin or chymotrypsin, and immunoblotted with these antibodies. The protease-resistant TDP-43 bands and smears were detected in ALS and all subtypes of FTLD-TDP with these anti-TDP-43 antibodies (Fig. 4), while no such bands were seen in AD cases. These demonstrate that the epitope is protease-resistant in the abnormal TDP-43 but not in normal TDP-43. Using an antibody pS409/410 that recognizes the C-terminal phosphorylation sites, some protease-resistant TDP-43 bands are detected, and the band patterns are slightly different between ALS and FTLD-TDP type C [29]. On immunoblots with anti-TDP-43 pAb and mAb, such difference was not observed. This is probably due to that the epitope of the mAb and pAb is located in the amino-terminus of the protease-resistant core of the TDP-43, whereas epitope of the pS409/410 located in the C-terminus. Similar protease-resistant bands have been reported in abnormal prion in prion diseases, tau in Alzheimer's disease and alpha-synuclein in Parkinson's disease and dementia with Lewy bodies. Biochemical studies in these proteinopathies suggested that the protease-resistant bands represent the core domains of the filamentous aggregates of these proteins with cross-β structures [30–32]. By analogy with these proteins we propose that these protease-resistant C-terminal fragments represent the core of the filamentous aggregates of TDP-43. Since the epitope of the mAb and pAb are determined to locate at residues 203–209, this may be important in the formation of a core region of pathological TDP-43 aggregates which is common in all TDP-43 proteinopathies. Finally, the protease treatment used in this study may be useful for detection of the abnormal TDP-43 in brains of patients, animal models, culture cells and in vitro models with these anti-TDP-43 antibodies more specifically, as used for detection of abnormal prion proteins.

Acknowledgments

Authors thank Dr Tetsuaki Arai (Tsukuba University) for helpful advice and discussions. This work was supported by a Grant-in-Aid for Scientific Research (A) (to M.H., 11000624) from Ministry of Education, Culture, Sports, Science and Technology of Japan, and grants from Ministry of Health, Labor and Welfare of Japan (to M.H.).

References

[1] Y.M. Ayala, T. Misteli, F.E. Baralle, TDP-43 regulates retinoblastoma protein phosphorylation through the repression of cyclin-dependent kinase 6 expression, Proc. Natl. Acad. Sci. U.S.A. 105 (2008) 3785–3789.

[2] Y.M. Ayala, F. Pagani, F.E. Baralle, TDP43 depletion rescues aberrant CFTR exon 9 skipping, FEBS Lett. 580 (2006) 1339–1344.

[3] E. Buratti, F.E. Baralle, Multiple roles of TDP-43 in gene expression, splicing regulation, and human disease, Front. Biosci. 13 (2008) 867–878.

[4] S.H. Ou, F. Wu, D. Harrich, et al., Cloning and characterization of a novel cellular protein, TDP-43, that binds to human immunodeficiency virus type 1 TAR DNA sequence motifs, J. Virol. 69 (1995) 3584–3596.

[5] I.F. Wang, N.M. Reddy, C.K. Shen, Higher order arrangement of the eukaryotic nuclear bodies, Proc. Natl. Acad. Sci. U.S.A. 99 (2002) 13583–13588.

[6] T. Arai, M. Hasegawa, H. Akiyama, et al., TDP-43 is a component of ubiquitin-positive tau-negative inclusions in frontotemporal lobar degeneration and amyotrophic lateral sclerosis, Biochem. Biophys. Res. Commun. 351 (2006) 602–611.

[7] M. Neumann, D.M. Sampathu, L.K. Kwong, et al., Ubiquitinated TDP-43 in frontotemporal lobar degeneration and amyotrophic lateral sclerosis, Science 314 (2006) 130–133.

[8] T. Arai, I.R. Mackenzie, M. Hasegawa, et al., Phosphorylated TDP-43 in Alzheimer's disease and dementia with Lewy bodies, Acta Neuropathol. (Berl) 117 (2009) 125–136.

[9] M. Hasegawa, T. Arai, H. Akiyama, et al., TDP-43 is deposited in the Guam parkinsonism-dementia complex brains, Brain 130 (2007) 1386–1394.

[10] C.F. Tan, M. Yamada, Y. Toyoshima, et al., Selective occurrence of TDP-43-immunoreactive inclusions in the lower motor neurons in Machado-Joseph disease, Acta Neuropathol. (Berl) 118 (2009) 553–560.

[11] Y. Toyoshima, H. Tanaka, M. Shimohata, et al., Spinocerebellar ataxia type 2 (SCA2) is associated with TDP-43 pathology, Acta Neuropathol. (Berl) 122 (2011) 375–378.

[12] O. Yokota, Y. Davidson, E.H. Bigio, et al., Phosphorylated TDP-43 pathology and hippocampal sclerosis in progressive supranuclear palsy, Acta Neuropathol. (Berl) 120 (2010) 55–66.

[13] E. Kabashi, P.N. Valdmanis, P. Dion, et al., TARDBP mutations in individuals with sporadic and familial amyotrophic lateral sclerosis, Nat. Genet. 40 (2008) 572–574.

[14] J. Sreedharan, I.P. Blair, V.B. Tripathi, et al., TDP-43 mutations in familial and sporadic amyotrophic lateral sclerosis, Science 319 (2008) 1668–1672.

[15] A. Tamaoka, M. Arai, M. Itokawa, et al., TDP-43 M337V mutation in familial amyotrophic lateral sclerosis in Japan, Intern. Med. 49 (2010) 331–334.

[16] I.R. Mackenzie, R. Rademakers, M. Neumann, TDP-43 and FUS in amyotrophic lateral sclerosis and frontotemporal dementia, Lancet Neurol. 9 (2010) 995–1007.

[17] M. Hasegawa, T. Arai, T. Nonaka, et al., Phosphorylated TDP-43 in frontotemporal lobar degeneration and amyotrophic lateral sclerosis, Ann. Neurol. 64 (2008) 60–70.

[18] I.R. Mackenzie, E.H. Bigio, P.G. Ince, et al., Pathological TDP-43 distinguishes sporadic amyotrophic lateral sclerosis from amyotrophic lateral sclerosis with SOD1 mutations, Ann. Neurol. 61 (2007) 427–434.

[19] M. Neumann, L.K. Kwong, A.C. Truax, et al., TDP-43-positive white matter pathology in frontotemporal lobar degeneration with ubiquitin-positive inclusions, J. Neuropathol. Exp. Neurol. 66 (2007) 177–183.

[20] H. Zhang, C.F. Tan, F. Mori, et al., TDP-43-immunoreactive neuronal and glial inclusions in the neostriatum in amyotrophic lateral sclerosis with and without dementia, Acta Neuropathol. (Berl) 115 (2008) 115–122.

[21] M. Neumann, I.R. Mackenzie, N.J. Cairns, et al., TDP-43 in the ubiquitin pathology of frontotemporal dementia with VCP gene mutations, J. Neuropathol. Exp. Neurol. 66 (2007) 152–157.

[22] H.X. Zhang, K. Tanji, F. Mori, et al., Epitope mapping of 2E2-D3, a monoclonal antibody directed against human TDP-43, Neurosci. Lett. 434 (2008) 170–174.

[23] T. Nonaka, F. Kametani, T. Arai, et al., Truncation and pathogenic mutations facilitate the formation of intracellular aggregates of TDP-43, Hum. Mol. Genet. 18 (2009) 3353–3364.

[24] T. Nonaka, T. Arai, E. Buratti, et al., Phosphorylated and ubiquitinated TDP-43 pathological inclusions in ALS and FTLD-U are recapitulated in SH-SY5Y cells, FEBS Lett. 583 (2009) 394–400.

[25] Y. Nishimoto, D. Ito, T. Yagi, et al., Characterization of alternative isoforms and inclusion body of the TAR DNA-binding protein-43, J. Biol. Chem. 285 (2010) 608–619.

[26] E. Buratti, F.E. Baralle, Characterization and functional implications of the RNA binding properties of nuclear factor TDP-43, a novel splicing regulator of CFTR exon 9, J. Biol. Chem. 276 (2001) 36337–36343.

[27] H. Wils, G. Kleinberger, J. Janssens, et al., TDP-43 transgenic mice develop spastic paralysis and neuronal inclusions characteristic of ALS and frontotemporal lobar degeneration, Proc. Natl. Acad. Sci. U.S.A. 107 (2010) 3858–3863.

[28] L.M. Igaz, L.K. Kwong, A. Chen-Plotkin, et al., Expression of TDP-43 C-terminal Fragments in Vitro Recapitulates Pathological Features of TDP-43 Proteinopathies, J. Biol. Chem. 284 (2009) 8516–8524.

[29] M. Hasegawa, T. Nonaka, H. Tsuji, et al., Molecular Dissection of TDP-43 Proteinopathies, J. Mol. Neurosci. 45 (2011) 480–485.

[30] J. Collinge, K.C. Sidle, J. Meads, et al., Molecular analysis of prion strain variation and the aetiology of 'new variant' CJD, Nature 383 (1996) 685–690.

[31] H. Miake, H. Mizusawa, T. Iwatsubo, et al., Biochemical characterization of the core structure of alpha-synuclein filaments, J. Biol. Chem. 277 (2002) 19213–19219.

[32] M. Novak, J. Kabat, C.M. Wischik, Molecular characterization of the minimal protease resistant tau unit of the Alzheimer's disease paired helical filament, EMBO J. 12 (1993) 365–370.

The FASEB Journal • Research Communication

Phosphorylated α-synuclein can be detected in blood plasma and is potentially a useful biomarker for Parkinson's disease

Penelope G. Foulds,* J. Douglas Mitchell,‡ Angela Parker,‡ Roisin Turner,‡ Gerwyn Green,† Peter Diggle,† Masato Hasegawa,§ Mark Taylor,* David Mann,‖ and David Allsop*,[1]

*Division of Biomedical and Life Sciences and †Division of Health Research, School of Health and Medicine, University of Lancaster, Lancaster, UK; ‡Royal Preston Hospital, Preston, UK; §Department of Molecular Neurobiology, Tokyo Institute of Psychiatry, Tokyo, Japan; and ‖Neurodegeneration and Mental Health Research Group, School of Community-Based Medicine, University of Manchester, Hope Hospital, Salford, UK

ABSTRACT **Parkinson's disease (PD) is characterized by the presence of Lewy bodies containing phosphorylated and aggregated α-synuclein (α-syn). α-Syn is present in human body fluids, including blood plasma, and is a potential biomarker for PD. Immunoassays for total and oligomeric forms of both normal and phosphorylated (at Ser-129) α-syn have been used to assay plasma samples from a longitudinal cohort of 32 patients with PD (sampled at mo 0, 1, 2, 3), as well as single plasma samples from a group of 30 healthy control participants. The levels of α-syn in plasma varied greatly between individuals, but were remarkably consistent over time within the same individual with PD. The mean level of phospho-α-syn was found to be higher (P=0.053) in the PD samples than the controls, whereas this was not the case for total α-syn (P=0.244), oligo-α-syn (P=0.221), or oligo-phospho-α-syn (P=0.181). Immunoblots of plasma revealed bands (at 21, 24, and 50–60 kDa) corresponding to phosphorylated α-syn. Thus, phosphorylated α-syn can be detected in blood plasma and shows more promise as a diagnostic marker than the nonphosphorylated protein. Longitudinal studies undertaken over a more extended time period will be required to determine whether α-syn can act as a marker of disease progression.—Foulds, P. G., Mitchell, J. D., Parker, A., Turner, R., Green, G., Diggle, P., Hasegawa, M., Taylor, M., Mann, D., Allsop, D. Phosphorylated α-synuclein can be detected in blood plasma and is potentially a useful biomarker for Parkinson's disease. *FASEB J.* 25, 4127–4137 (2011). www.fasebj.org**

Key Words: Lewy body · oligomer · immunoassay · immunoblot

PARKINSON'S DISEASE (PD) is the second most common neurodegenerative disorder after Alzheimer's disease (AD) and is characterized clinically by the 3 cardinal motor symptoms of resting tremor, rigidity, and bradykinesia. Patients often exhibit further symptoms, including postural imbalance, gait disturbance, and a mask-like facial expression. In the advanced stages of PD, nonmotor symptoms can also appear, including anxiety, depression, dementia, and psychosis. The defining neuropathological features of idiopathic PD are the loss of dopaminergic neurons from the substantia nigra (SN) and the presence of Lewy bodies (LBs) and Lewy neurites (LNs) in surviving neurons of this and other brain regions (1). Similar lesions are present within the cerebral cortex in the related disorder of dementia with Lewy bodies (DLB; ref. 2). LBs and LNs contain a misfolded, fibrillar, and phosphorylated form of the protein α-synuclein (α-syn; refs. 1, 3). Pathological changes involving α-syn, chiefly in glial cells, also occur in multiple system atrophy (MSA), and, therefore, PD, DLB, and MSA are often collectively referred to as "α-syncleinopathies" (2). Duplication (4, 5), triplication (6), and mutation (7–9) of the gene encoding α-syn (*SNCA*) are all causes of hereditary forms of either PD or DLB. α-Syn oligomers are believed to be toxic to cells, as are oligomers derived from the various proteins associated with several other protein-misfolding neurodegenerative disorders, such as AD or the prion disorders (10, 11). Overexpression of wild-type or mutant α-syn in animal models can produce a phenotype resembling PD, including SN degeneration, movement problems and responsiveness to L-dopa therapy (12–15). Together, these observations suggest that α-syn plays a pivotal role in the development of the α-synucleinopathies (16).

PD is one of several neurological movement disor-

[1] Correspondence: Division of Biomedical and Life Sciences, School of Health and Medicine, University of Lancaster, Lancaster, LA1 4AY, UK. E-mail: d.allsop@lancaster.ac.uk

doi: 10.1096/fj.10-179192

This article includes supplemental data. Please visit *http://www.fasebj.org* to obtain this information.

ders that can produce similar symptoms, and a correct diagnosis is critically dependent on clinical examination to rule out disorders that can mimic PD. A diagnosis of PD is considered if the person exhibits more than one of the 3 cardinal motor symptoms mentioned above (17). The presence of resting tremor supports the diagnosis of PD more than the other two symptoms, but ~20% of patients with autopsy-confirmed PD fail to develop any resting tremor (18). Moreover, only 69–70% of people with autopsy-confirmed PD have at least two of the cardinal signs of the disease and 20–25% of people with two of these symptoms have a pathological diagnosis other than PD (19, 20). Perhaps even more surprising is the finding that 13–19% of people who demonstrate all three of the cardinal features have a pathological diagnosis other than PD (19, 20). Because the progression of neurological movement disorders and their treatment varies greatly, proper clinical diagnosis is essential for correct patient management. Furthermore, by the time PD is diagnosed, >60% of dopaminergic neurons in the SN can already be lost (21), making accurate early diagnosis, ideally before clinical symptoms appear, essential for any effective neuroprotective intervention strategy. Also, the clinical diagnosis of early PD may be difficult because although the patient might complain of symptoms suggesting PD, the neurological examination may be normal (22). These problems with clinical diagnosis have led to an increased interest in the development of diagnostic markers for PD, including advanced brain imaging methodologies (23) and molecular biomarkers (24). Genetic testing for mutations in genes linked to familial PD (including *SNCA*) is available (25), but it is only relevant when there is a strong family history, or when symptoms present at an unusually young age.

We have reported that α-syn is released from cells and is present in human body fluids, including cerebrospinal fluid (CSF) and blood plasma (26). This extracellular form of α-syn seems to be secreted from neuronal cells by exocytosis (27, 28) and could play an important role in cell-to-cell transfer of α-syn pathology in the brain (29). There is now an emerging consensus that the levels of α-syn are, on average, lower in samples of CSF taken from a group of patients with PD compared with a group of normal or neurological controls (30, 31), especially when the confounding variables of age and blood contamination are taken into account (32, 33). However, obtaining CSF is an invasive procedure, and analysis of α-syn levels in CSF is not generally amenable to longitudinal study. There are also some studies of α-syn as a potential biomarker in the much more accessible peripheral blood, with an initial report suggesting increased levels of this protein in plasma samples from patients with PD compared with those from healthy controls (34). However, subsequent studies have reported decreased levels of α-syn in PD plasma (35) or no significant change (36). We have shown that the levels of oligomeric α-syn appear to be significantly elevated in plasma samples from a group of patients with PD compared with a group of diseased controls (37). To develop this line of enquiry further, we have now set up a longitudinal study in newly diagnosed patients with PD to examine the levels of various different forms of α-syn, including phosphorylated and/or oligomeric forms, in blood plasma. Because α-syn accumulates in a phosphorylated and aggregated form in LBs (3), it is possible that these modified, pathological forms of the protein will more accurately reflect the fundamental neuropathology of PD than straightforward measures of "total" α-syn (33, 38). Our ultimate aim is to develop a relatively simple test for the early diagnosis of PD, or a surrogate marker for monitoring the progression of PD. Here, we report the results obtained during the initial phase of this longitudinal study.

MATERIALS AND METHODS

Patient population and clinical method

Participants for this study were recruited (with ethical approval, using appropriate consenting procedures) from the neurological service based at the Royal Preston Hospital along with other similar departments in the northwest of England. The diagnosis of PD was based on the UK Parkinson's Disease Society diagnostic criteria for PD (39). Severity of disease was defined in terms of patients satisfying the criteria for stages 1 or 2 on the Hoehn and Yahr scale.

The overall target for the study was to follow a cohort of 200 patients meeting these criteria over a period of 2–3 yr, reviewing them at 4- to 6-mo intervals. This study is ongoing, but the plan was also to follow the first 32 patients more intensively over the initial phases of the study, and this group was seen at monthly intervals for the first 3 mo. The results from these 32 patients over the first 3 mo are presented here. Blood samples were obtained from the participating sites (Preston and Arrowe Park). Around 3 ml of blood was collected in tubes containing EDTA, and the plasma was separated within 3 h by centrifuging the blood at 3000 *g* for 10 min. The plasma was immediately stored at −80°C. Appropriate care was taken to avoid contamination of the plasma samples with cells or components of the pellet obtained from the centrifugation. The samples were thawed at room temperature directly before analysis. Repeated freeze/thaw cycles were avoided.

Control subjects were healthy individuals with no apparent neurological or known psychiatric symptoms who were the spouses of patients attending the Cerebral Function Unit clinics at Hope Hospital (Salford Royal Hospital, National Health Service Foundation Trust) for investigation and diagnosis of dementia. These control subjects were recruited as part of an ongoing investigation into the genetics and molecular biology of dementia approved by the Oldham Local Research Ethics Committee. Blood plasma was prepared and stored as described above.

Preparation of recombinant α-syn

Recombinant α-syn (without any purification tag) was prepared at Lancaster University from *Escherichia coli* using the following protocol. pJEK2 was used to transform FB850, a *rec* A^- derivative of BL21 (DES) pLysS. FB850 carrying this plasmid was grown in an 800-ml batch culture, and protein expression was induced through the addition of isopropyl-β-

D-thiogalactopyranoside (IPTG). A protein with a molecular weight of ~17 kDa started to accumulate in the cells 30 min after induction and reached maximum levels after 150 min. Immunoblot analysis identified this protein as α-syn using an anti-α-syn mouse monoclonal antibody (MAb 211; Santa Cruz Biotechnology, Santa Cruz, CA, USA). After a 3-h induction, the suspension was centrifuged, and the cells were resuspended in buffer. The cells were lysed by sonication, and then cell debris and insoluble material were removed by centrifugation at 4°C for 1 h at 30,000 rpm. α-Syn was extracted from the supernatant by ammonium sulfate precipitation, then purified using two chromatography columns; mono Q and Superdex 200 (Amersham Biosciences, Piscataway, NJ, USA). After purification, 5 μg of protein ran as a single band when observed on a Coomassie blue-stained SDS gel, corresponding to monomeric α-syn.

Preparation of phosphorylated recombinant α-syn

Phosphorylated α-syn was prepared from recombinant α-syn, as described previously (40). Briefly, α-syn (630 μM) was incubated with casein kinase II (CK2; New England Biolabs, Ipswitch, MA, USA) in 1 ml of buffer containing 20 mM Tris-HCl (pH 7.5), 50 mM KCl, 10 mM $MgCl_2$, and 1 mM ATP at 30°C for 24 h. For effective phosphorylation, CK2 was added to the reaction mixture at 2-h intervals for the first 10 h (7500 U×5). The reaction was stopped by boiling for 5 min, cleared by centrifugation at 113,000 *g* for 20 min at 4°C, and then loaded onto a Resource Q anion-exchange column (Amersham Biosciences) equilibrated with 20 mM Tris-HCl (pH 8.0) and 0.2 M NaCl, and then eluted with a linear gradient of NaCl from 0.20 to 0.35 M for 15 min at a flow rate of 1 ml/min. Fractionated samples were analyzed by immunoblotting with a phosphorylation-dependent anti-α-syn antibody, PSer129 (Epitomics, Burlingame, CA, USA), and mass spectrometry. The PSer129-positive phosphorylated α-syn recovered in the fractions with ~0.3 M NaCl was concentrated by ammonium sulfate precipitation.

Preparation of oligomeric forms of recombinant α-syn

To prepare a standard for the oligomeric α-syn immunoassay, the recombinant protein was oligomerized by incubation at 45 μM in PBS in an orbital shaker at 37°C for 5 d, and the monomer and oligomer were separated by size-exclusion chromatography. A sample (0.5 ml) of preaggregated α-syn was loaded onto a Superdex 200 column (44×1 cm) connected to a fast protein liquid chromatography (FPLC) system (Atka Purifier; GE Healthcare, New York, NY, USA) and eluted with running buffer (PBS) at a flow rate of 0.5 ml/min. Absorbance of the eluate was monitored at 280 nm; fractions of 1 ml were collected, and protein concentration was determined.

To prepare a standard for the oligo-phospho-α-syn immunoassay, the phosphorylated protein was oligomerized by incubation at 50 μM in PBS in an orbital shaker at 37°C for 5 d. Aggregation of the protein was confirmed by thioflavin T assay. In this case, the amount of sample available was too small to fractionate by size-exclusion chromatography.

Immunoassay methods

We have already established immunoassay methods for the measurement of total and soluble oligomeric forms of α-syn in human biological fluids, including blood plasma (37, 41), and these methods have been further optimized.

Total α-syn

A 96-well microtiter plate (Iwaki, Holliston, MA, USA) was coated with 100 μl/well of anti-α-syn monoclonal antibody 211 diluted 1:1000 (0.2 μg/ml; Santa Cruz Biotechnology) in 50 mM $NaHCO_3$ (pH 9.6) and incubated at 4°C overnight. The wells were then washed 4 times with PBS containing 0.05% Tween-20 (PBS-T) and were incubated for 2 h at 37°C with 200 μl/well of freshly prepared blocking buffer (2.5% gelatin in PBS-T). The plate was washed again 4 times with PBS-T, and 100 μl of the assay standard or plasma samples was added to each well (each plasma sample was diluted 1:40 with PBS), and the assays were performed in triplicate. Following this, the plate was incubated at 37°C for 2 h. After a repeat washing with PBS-T, 100 μl/well of the detection antibody, anti-α/β/γ-synuclein FL-140 (Santa Cruz Biotechnology), dilution 1:750 (0.27 μg/ml) in blocking buffer was added, and the plate was incubated at 37°C for 2 h. After another wash with PBS-T, the plate was incubated with 100 μl/well of secondary antibody [goat anti-rabbit horseradish peroxidase (HRP); Sigma, St. Louis, MO, USA], dilution 1:10,000 in blocking buffer at 37°C for 2 h. The plate was then washed again with PBS-T before adding 100 μl/well of Sure Blue TMB microwell peroxidase substrate (KPL, Gaithersburg, MD, USA) and leaving the color to develop for 30 min at room temperature. Finally 100 μl/well of stop solution (0.3 M H_2SO_4) was added, and absorbance at 450 nm was determined. Recombinant monomeric α-syn was used to create a standard curve.

Oligomeric α-syn (oligo-α-syn)

The microtiter plate was coated and blocked using the same method as the assay for total α-syn. The wells were then washed 4 times with PBS-T, and 100 μl of the plasma sample (diluted 1:25 with PBS) or assay standard (oligo-α-syn) was added to each well, in triplicate. Following this, the plate was incubated at 37°C for 2 h. After a repeat wash with PBS-T, 100 μl/well of the detection antibody, biotinylated anti-α-synuclein 211 (diluted 1:1000 in blocking buffer) was added, and the plate was incubated at 37°C for 2 h. After another wash with PBS-T, the plate was incubated with 100 μl/well of streptavidin-europium, diluted 1:500 in streptavidin-europium buffer (Perkin Elmer, Wellesley, MA, USA) and shaken for 10 min. After a further 50-min agitation on a rotating platform, the plate was washed again with PBS-T, before adding 100 μl/well enhancer solution (Perkin Elmer). Finally, the plates were read on a Wallac Victor^2 1420 multilabel plate reader (Perkin Elmer), using the time-resolved fluorescence setting for europium.

Total phosphorylated α-syn (pS-α-syn)

The antibody-sandwich ELISA for total α-syn was modified to detect only the protein phosphorylated at Ser-129 by replacing the 211 phospho-independent capture antibody with polyclonal anti-α-synuclein N-19 (Santa Cruz Biotechnology), diluted 1:3,000 (0.07 μg/ml). The phospho-dependent rabbit monoclonal antibody, Phospho (pS129) antibody (Epitomics), used at a dilution of 1:3000, was the chosen detection antibody. This antibody detects only α-syn phosphorylated at Ser-129. The preferred secondary antibody was human serum absorbed goat anti-rabbit HRP, 1:3000 (KPL), rehydrated in 1 ml H_2O. Recombinant pS-α-syn was used as the assay standard.

Oligomeric phosphorylated α-syn (oligo-pS-α-syn)

The antibody-sandwich immunoassay for oligo-α-syn was modified to detect only phosphorylated, oligomeric forms of the

protein, by replacing the 211 phospho-independent capture antibody with the phospho-dependent rabbit monoclonal antibody, pS129 (Epitomics), used at a dilution of 1:3000. The detection antibody was biotinylated pS129 at a dilution of 1:400. Recombinant oligo-pS-α-syn was used to generate a standard curve.

Preparation of biotinylated antibodies

To prepare the biotinylated antibody, 200 g Sulfo-NHS-LC-Biotin (Pierce, Rockford, IL, USA) was reacted with the required antibody (1 ml, 200 μg/ml) in PBS and then placed on ice for 2 h. The mixture was desalted on Bio-Spin-6 columns (Bio-Rad, Richmond, CA, USA) to remove excess uncoupled biotin and the biotinylated antibody was stored at −20°C until use.

Immunocapture of α-syn from plasma

Dynabeads covalently coupled with recombinant protein G were derivatized with goat polyclonal anti-α-syn synuclein N-19 antibody (Santa Cruz Biotechnology), as recommended by the manufacturer (Dynal Biotech, Wirral, UK). Plasma (500 μl) was added to the beads and incubated overnight at 4°C. The plasma samples were chosen according to the immunoassay results, with one sample giving a high signal for the phosphorylated protein, the other a low signal, and a control containing PBS only. The beads were then washed 3 times with 0.1 M phosphate buffer (pH 8.2). Any captured protein was eluted from the beads by boiling for 10 min in NuPAGE LDS sample buffer (Invitrogen, Carlsbad, CA, USA) and was examined by gel electrophoresis and immunoblotting.

Gel electrophoresis and immunoblotting

The protein eluted from the magnetic Dynabeads was separated on 12.5% acylamide gels. The separated proteins were transferred to nitrocellulose membranes (0.45 μm, Invitrogen) at 30 V, 125 mA for 1 h. Membranes were blocked with 5% dried skimmed milk dissolved in PBS-Tween (PBST), for 1 h. The membranes were probed overnight at 4°C with either phospho-dependent rabbit anti-α-synuclein monoclonal antibody pS129 (Epitomics) at a dilution of 1:5000; rabbit polyclonal anti-synuclein antibody FL-140 (Santa Cruz Biotechnology) at a dilution of 1:1000 (0.2 μg/ml); or rabbit anti-ubiquitin antibody FL-76 (Santa Cruz Biotechnology) at a dilution of 1:1000 (0.2 μg/ml) in PBST. The membranes were washed 3 times in PBST, followed by incubation with human serum absorbed HRP-conjugated goat anti-rabbit (Sigma), 1:10,000 in PBST, for 1 h. The protein bands were visualized using ECL reagents (Pierce), as described by the manufacturer.

Analysis of immunoassay data

A set of standards for one of the 4 different assays (*i.e.*, for total α-syn, oligo-α-syn, pS-α-syn, or oligo-pS-α-syn) was included on each microtiter plate, as appropriate for the type of protein being measured on that plate. Standard curves were fitted using nonlinear least squares (see **Fig. 1** for representative examples of standard curves for each of the four different immunoassays). The samples of blood plasma from

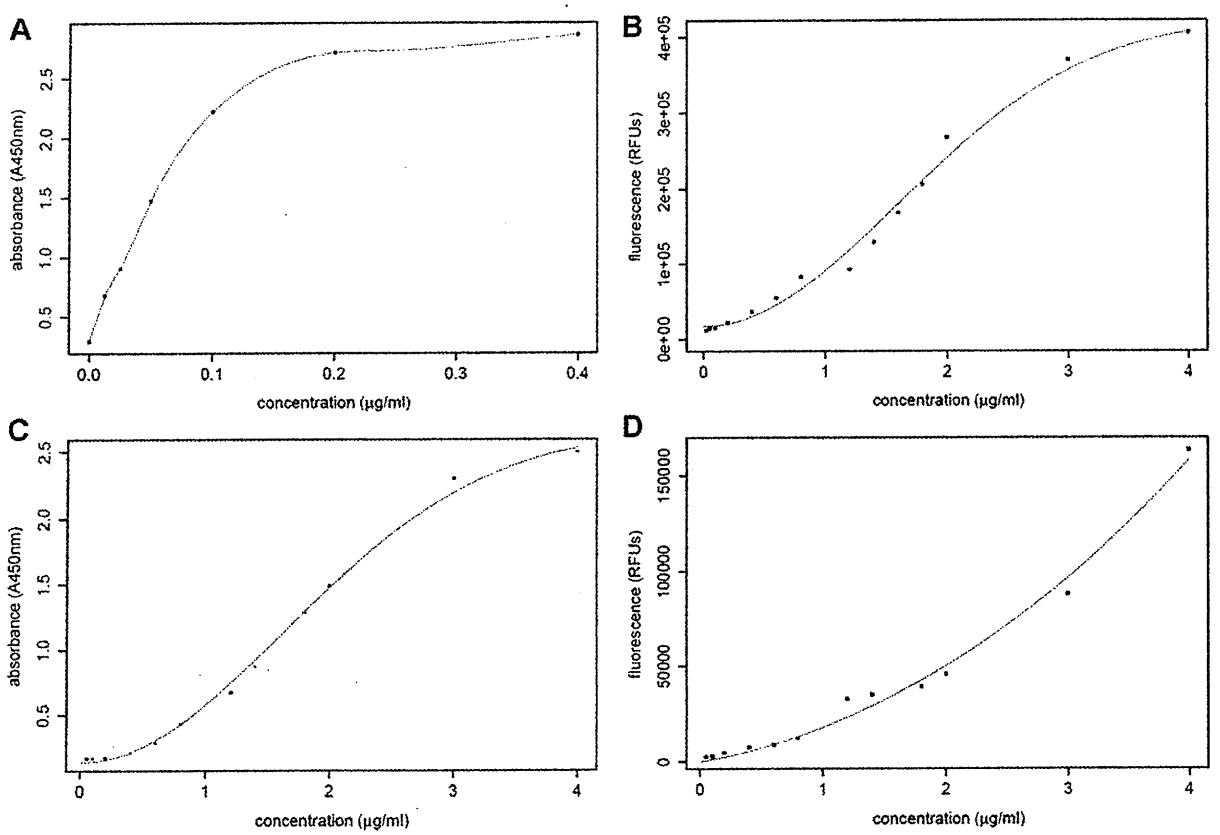

Figure 1. Examples of standard curves obtained for total α-syn (*A*), oligo-α-syn (*B*), pS-α-syn (*C*) and oligo-pS-α-syn (*D*). These are representative curves, each obtained from a single ELISA plate.

patients with PD and controls, diluted as indicated above, were measured in triplicate for each individual at each time point. The standard curves for each individual plate were used to transform the absorbance values (total α-syn, pS-α-syn) or relative fluorescence units (RFU; oligo-α-syn, oligo-pS-α-syn) for that particular plate into protein concentrations, and, in this way, any variation between plates was accounted for. The specificity of the oligo-α-syn immunoassay toward aggregated forms of α-syn has been reported previously (37, 41) but was confirmed here by analysis of fractions obtained by gel filtration of preaggregated, recombinant α-syn; only the peak containing α-syn oligomers, and not the monomer peak, was detected by the oligo-α-syn immunoassay. Also, as expected, the nonphosphorylated form of α-syn gave no signal in the pS-α-syn immunoassay, and the oligo-pS-α-syn immunoassay detected only pS-α-syn that had been preaggregated (data not shown). Further, when the blood plasma samples were immunodepleted with anti-α-syn antibodies C211 or FL-140, each coupled to magnetic Dynabeads, and then tested in the immunoassays, only trace signals could be detected above background compared to the nonimmunodepleted samples (data not shown).

To investigate whether the protein levels changed over time (*i.e.*, during the first 3 mo) a linear mixed model was fitted to the longitudinal data from each assay (details in Supplemental Data).

A classic 2-sample *t* test was used to determine whether there was any significant difference between the mean levels of each of the different forms of α-syn when comparing the plasma samples from the patients with PD with those from the healthy controls. To better satisfy the assumptions underlying this test, the empirical distributions were constructed on the logarithmic scale to obtain a more symmetric distribution than was obtained on the original scale.

RESULTS

Patient population and demographics

Demographic details of the cohort of 32 patients with PD that was followed at monthly intervals for 3 mo are summarized in **Table 1**. The mean age of this cohort on ascertainment and initial sampling was 68.2 yr (youngest 56 yr, oldest 85 yr). Among the 30 recruited healthy controls, there were 13 males and 17 females, with a median age of 63 yr and mean age of 61.5 yr (youngest 42 yr, oldest 75 yr). The PD case and control subjects were recruited in parallel, at the same clinical centers, and the blood samples were taken and processed by the same personnel at each site. Moreover, the plasma samples were effectively randomized for analysis, with both control and PD samples being assayed together on the same microtiter plates.

TABLE 1. *Demographic details of the cohort of 32 patients with PD*

Parameter	Value
Gender (male/female)	23/9
Hoehn and Yahr 1.0	5
Hoehn and Yahr 1.5	3
Hoehn and Yahr 2.0	24
Median PD onset age (yr)	61.9 (55.5–69.7)
Age at study recruitment (yr)	68.4 (62.3–73.8)
Disease duration at study recruitment (yr)	4.9 (3.1–9.3)

Values in parentheses indicate interquartile range.

Longitudinal data from patients with PD

Figure 2 presents a bar plot of the total α-syn plasma concentrations for each individual with PD over time (*i.e.*, for mo 0, 1, 2, 3) where, within each time point, we have averaged over triplicate measurements. It can be seen that the levels of total α-syn varied greatly between individuals, within an overall range of 0.01–6 μg/ml. Although a few individuals did show small, stepwise increases or decreases of total α-syn levels over this (very short) sampling period (see, for example, patient 32 in Fig. 2*B*), one of the most striking findings from this study was that, overall, the immunoassay results from the repeat PD plasma samples were remarkably consistent within each individual over time. This was a general finding for the results from all four of the different α-syn immunoassays, but it is illustrated here (Fig. 2) for the total-α-syn data only. Data for the other 3 assays (Supplemental File S2), together with a linear mixed model-based analysis (Supplemental File S1) for all 4 α-syn assays, are available in Supplemental Data. From the latter analysis, it is clear that the variation in α-syn levels across time within an individual is negligible relative to the variation across individuals. The model specifies a time trend, in addition to accounting for inherent differences in protein levels between individuals and differences across time within an individual. In all cases, the confidence interval for the estimated temporal effect covered 0. Thus, we conclude that there was no significant change over time for the levels of α-syn being measured by any of the immunoassays.

Comparison of patients with PD and controls

Empirical distributions of the α-syn concentrations for each assay were highly skewed on the original scale. **Figure 3** presents box plots pertaining to each assay, stratified according to patients with PD and controls. Note that the whiskers of the box plots extend by no more than the range of the data (largest minus smallest value) multiplied by the interquartile range. Extending the whiskers to the largest and smallest values would yield a rather compressed box. An apparent feature of the box plots is that the median concentration of α-syn for the patients exceeds that of the controls for both of the assays for phosphorylated α-syn (*i.e.*, pS-α-syn in Fig. 3*B*, and oligo-pS-α-syn in Fig. 3*D*). The reverse is true regarding the nonphosphorylated assays (total-α-syn in Fig. 3*A* and oligo-α-syn in Fig. 3*C*). Further, the interquartile range (*i.e.*, box height) reports that the concentrations are far less dispersed for controls compared to patients for both of the phosphorylated α-syn assays. For the nonphosphorylated assays, the controls display a larger spread of concentrations.

To investigate the potential of α-syn as a means of

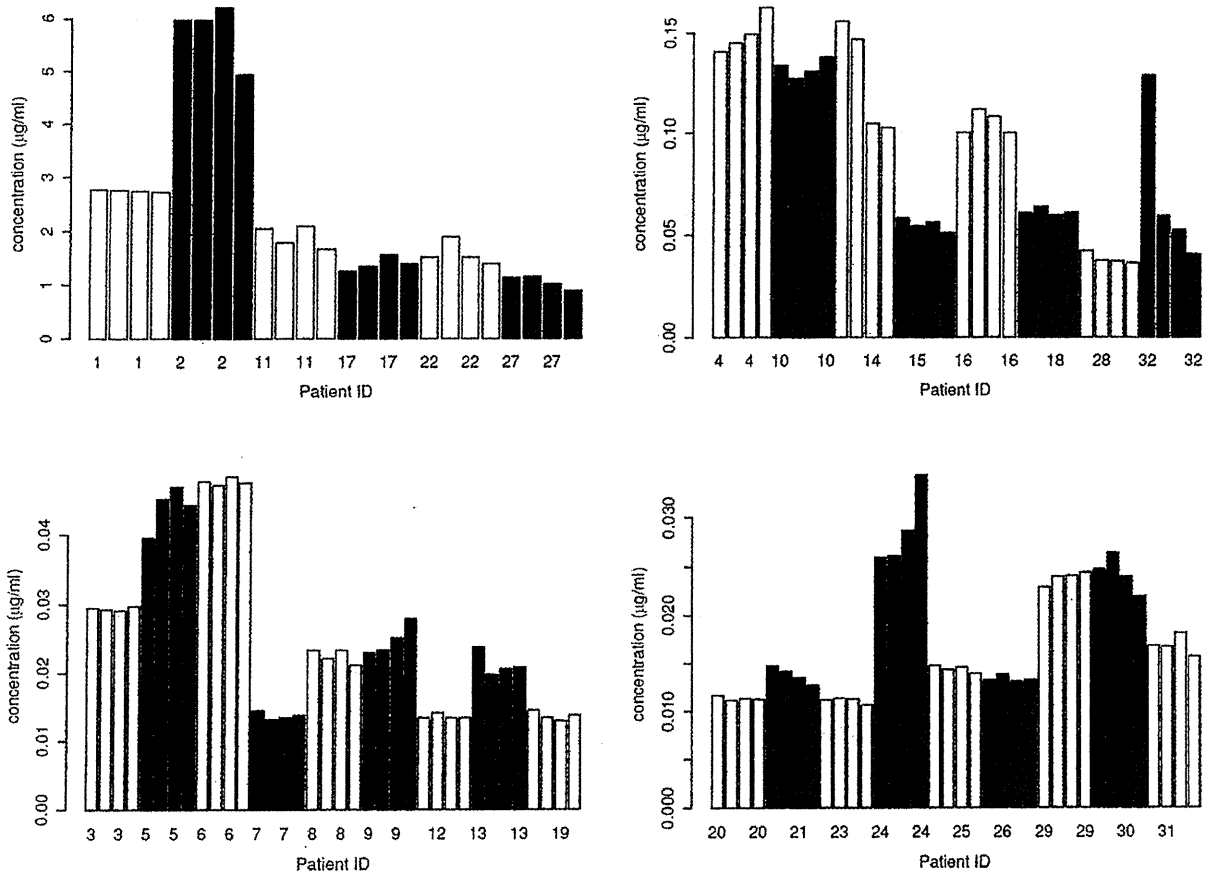

Figure 2. Longitudinal data for the levels of total α-syn in plasma samples from all of the 32 patients with PD. Consecutive bars for each patient represent the level of total α-syn in blood plasma samples taken at 0, 1, 2 and 3 mo. The participants are assigned to one of the 4 sections depending on their overall levels of protein.

discriminating between patients with PD and controls, we determined whether there was any significant difference between the average level of α-syn (on the logarithmic scale) across patients and controls, within all 4 α-syn assays. Because there was no consistent change in α-syn levels over time, nor across replicates within time, in the plasma samples from patients with PD, the concentrations for mo 0, 1, 2 and 3 were averaged over time and replicates in order to obtain a single mean value for each individual patient. Under a classical two-sample *t* test, the mean level of pS-α-syn was found to be marginally significantly higher for the patients than for the healthy controls (P=0.053). On the other hand, there was no difference across the average levels of patients and controls with regard to total α-syn (P=0.244), oligo-α-syn (P=0.221), or oligo-pS-α-syn (P=0.181).

Association with gender and age

The levels of α-syn showed no association with gender. For the total and oligo-α-syn assays, sampling age was a marginally significant −0.049 (−0.099, −0.001; P=0.052) and significant −0.009 (−0.019, −0.001; P=0.045) predictor, respectively, of α-syn levels in the patients with PD. On the other hand, the P values corresponding to the effect of sampling age on α-syn levels in the patients, under the pS-α-syn and oligo-pS-α-syn assays, were 0.412 and 0.274, respectively. The levels of α-syn showed no correlation with age in the control group. We did also analyze the data adjusting for age, but found no significant effects, and the adjustments did not materially change the (lack of) significance of the relevant assay results. Therefore, we chose to report the unadjusted results for simplicity.

Receiver operating curve (ROC) analysis

Figure 4 displays an ROC curve constructed to evaluate the utility of plasma pS-α-syn levels in discriminating patients with PD from healthy controls. The area under the curve (AUC) of 0.68 suggests that pS-α-syn has some potential value as a discriminant between patients and controls. AUC curves for 2 of the other 3 assays gave AUC values of less than 0.5 (0.28 for total α-syn and 0.22 for oligo-α-syn), which would also indicate a potentially informative result, with plasma levels of these being lower in patients than in controls. An AUC of 0.62 for oligo-pS-α-syn, however, suggests that in this

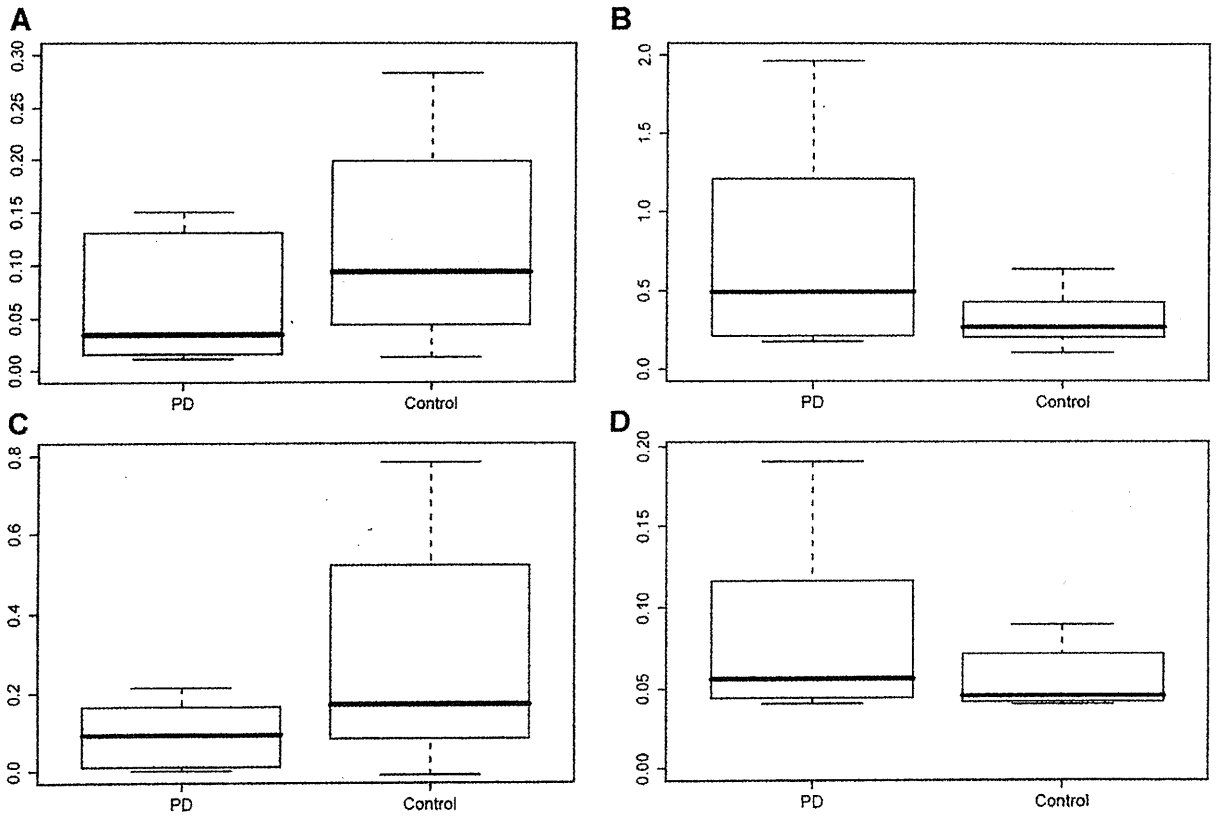

Figure 3. Box plots comparing the levels (in μg/ml) of total α-syn (*A*), pS-α-syn (*B*), oligo-α-syn (*C*), and oligo-pS-α-syn (*D*) in patients with PD compared to healthy controls. In each plot, the box extends from the lower to the upper quartile of the data, with the median indicated by a horizontal line within the box. The difference between the lower and upper quartiles is called the interquartile range (IQR). The upper and lower whiskers extend to the most extreme data values that are no more than 1.5 IQR greater than the upper quartile, and no more than 1.5 IQR less than the lower quartile, respectively.

particular sample set, this assay is less likely to have any practical value as a discriminatory diagnostic tool.

Immunoblot analysis of phosphorylated α-syn in plasma

To better characterize the phosphorylated α-syn detected in plasma, we extracted α-syn from individual PD plasma samples by immunocapture on magnetic Dynabeads and then analyzed the extracted proteins by immunoblotting. The beads were derivatized with the phosphorylation-independent α-syn antibody N-19 (Santa Cruz Biotechnology), which is the antibody used for capture in the pS-α-syn immunoassay. Proteins eluted from the beads were detected by immunoblotting with two different α-syn antibodies: phosphorylation-dependent rabbit monoclonal antibody, pS129, which is the detection antibody used in the pS-α-syn immunoassay (**Fig. 5*A***), and the phosphorylation-independent rabbit polyclonal antibody, FL-140 (Fig. 5*B*). Rabbit anti-ubiquitin antibody FL-76 (Santa Cruz Biotechnology) was used to determine whether any of the bands represented ubiquitinated forms of α-syn (Fig. 5*C*).

The plasma samples were chosen according to the immunoassay results, with one sample giving a low signal for pS-α-syn (Fig. 5, lane 2) and the other a high signal (Fig. 5, lane 3). Immunoblots using the phospho-α-syn-dependent antibody revealed immunoreactive bands from both of these plasma samples, together with the human recombinant phospho-α-syn (at ~17 kDa), but not the nonphosphorylated recombinant protein (Fig. 5*A*, lane 4). The sample derived from the high-reading plasma revealed more intense bands than the low-reading sample, at ~21, 24, and 50–60 kDa. FL-140 revealed both the phosphorylated and nonphosphorylated recombinant protein standards, and also a 24-kDa band in both plasma samples (Fig. 5*B*). The 21-kDa band detected by pS129 was absent, but an additional higher-molecular-weight smear, at >35 kDa, was present. On the basis of the size of these α-syn species, we hypothesize that the 24-kDa band may correspond to phosphorylated, monoubiquitinated α-syn. The anti-ubiquitin antibody, FL-76, strongly labeled the 24-kDa band, as well as the broad "smears" at higher molecular mass, suggesting that all of these bands represent ubiquitinated forms of α-syn (Fig. 5*C*). Control samples of 100 ng human IgG and albumin, the N-19 immunocapture antibody, and a control immunoprecipitation

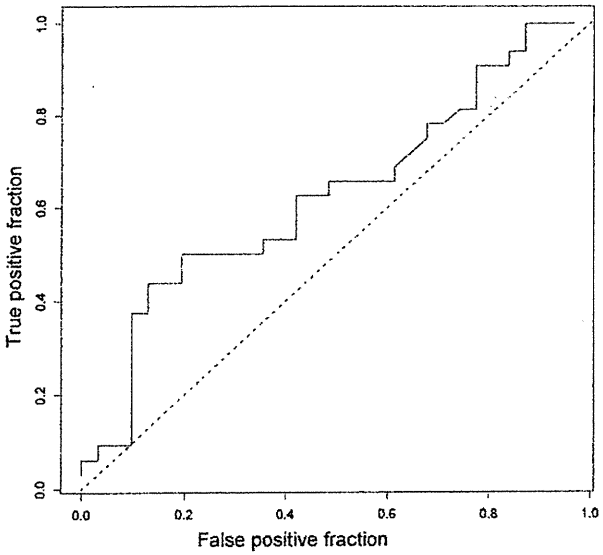

Figure 4. ROC curve showing the ability of the pS-α-syn levels to discriminate between patients with PD and healthy controls (AUC=0.68).

using PBS rather than plasma, gave no immunoreactive bands (data not shown).

DISCUSSION

α-Syn has been linked directly to the etiology of the α-synucleinopathies by mutations in and multiplication of its gene (*SNCA*) that result in familial forms of either PD or DLB. We have reported previously that α-syn is released from cells and is present in human body fluids, including CSF and blood plasma (26). This has led to considerable interest in α-syn in these body fluids as a potential biomarker for the α-synucleinopathies (30–37, 42–44). However, most of these studies have relied on immunoassays that cannot distinguish between monomeric/oligomeric and nonphosphorylated/phosphorylated forms of the protein, apart from two previous studies of oligomeric α-syn in human CSF or blood plasma (37, 44). Here, we have set up individual sandwich immunoassays that can distinguish between total α-syn (MAb 211 capture/ FL-140 detect); oligo-α-syn (Mab 211 capture and detect); pS-α-syn (N19 capture/pS129 detect); and oligo-pS-α-syn (pS129 capture and detect). Our assays for oligomeric forms of α-syn use the double-antibody approach, where the same monoclonal antibody is used for both antigen capture and detection (37, 41). This type of assay cannot detect monomers because the capture antibody occupies the only antibody-binding site available, but it can detect oligomers, because they have multiple binding sites. Our assays for phosphorylated α-syn rely on the specificity of the monoclonal antibody pS129 to α-syn phosphorylated at Ser-129 (45). As anticipated, the recombinant nonphosphorylated α-syn gave no signal in these assays. Although the absorbance/fluorescence values for each of the 4 assays were converted to protein concentrations using the relevant standard curve, due to the nature of these assays, this may only represent an estimate of concentration for that particular assay since the precise nature of the α-syn species detected in plasma has not been not determined for each assay and the native species are likely to differ from the standards prepared from the recombinant

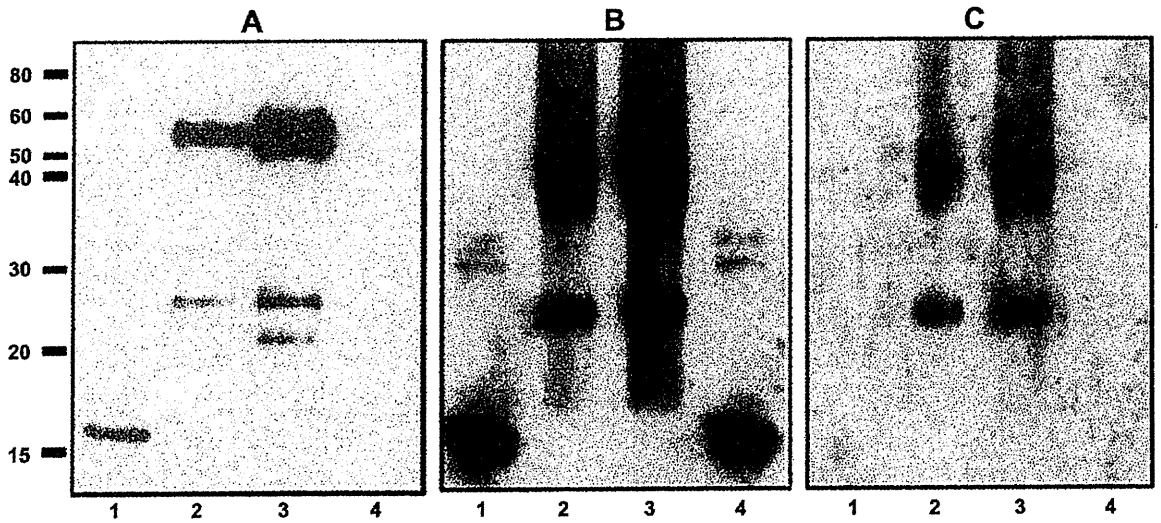

Figure 5. Immunoblot analysis of phosphorylated α-syn from plasma samples. Proteins immunocaptured from one plasma sample giving a low immunoassay signal for pS-α-syn protein (lane 2), and the other a high signal (lane 3), were immunoblotted along with recombinant phosphorylated α-syn (lane 1), and the recombinant nonphosphorylated standard (lane 4). *A*) Analysis with the phospho-dependent α-syn rabbit monoclonal antibody pS129 (Epitomics). *B*) Analysis with the rabbit polyclonal α-syn antibody FL-140 (Santa Cruz Biotechnology). Analysis with the rabbit polyclonal antiubiquitin antibody FL-76 (Santa Cruz Biotechnology).